Hippocampal protein aggregation signatures fully distinguish pathogenic and wildtype *UBQLN2* in amyotrophic lateral sclerosis

Kyrah M. Thumbadoo[1,2], Birger V. Dieriks[2,3], Helen C. Murray[2,3], Molly E. V. Swanson[1,3], Ji Hun Yoo[2,4], Nasim F. Mehrabi[2,3], Clinton Turner[2,3,5], Michael Dragunow[2,4], Richard L. M. Faull[2,3], Maurice A. Curtis[2,3], Teepu Siddique[6], Christopher E. Shaw[2,7], Lyndal Henden[8], Kelly L. Williams[8], Garth A. Nicholson[8,9,10,11], Emma L. Scotter[1,2]

1 School of Biological Sciences, University of Auckland, Auckland, New Zealand
2 Centre for Brain Research, University of Auckland, Auckland, New Zealand
3 Department of Anatomy and Medical Imaging, University of Auckland, Auckland, New Zealand
4 Department of Pharmacology and Clinical Pharmacology, University of Auckland, Auckland, New Zealand
5 Department of Anatomical Pathology, LabPlus, Auckland City Hospital, Auckland, New Zealand
6 Departments of Neurology, Cell and Developmental Biology and Pathology, Northwestern University Feinberg School of Medicine, Chicago, USA
7 UK Dementia Research Institute Centre, Institute of Psychiatry, Psychology and Neuroscience, King's College London, United Kingdom
8 Macquarie University Centre for Motor Neuron Disease Research, Macquarie Medical School, Faculty of Medicine, Health and Human Sciences, Macquarie University, Sydney, New South Wales, Australia
9 Northcott Neuroscience Laboratory, Australian and New Zealand Army Corps (ANZAC) Research Institute, Concord, New South Wales, Australia
10 Faculty of Medicine, University of Sydney, Sydney, New South Wales, Australia
11 Molecular Medicine Laboratory, Concord Repatriation General Hospital, Concord, New South Wales, Australia
12

Corresponding author:
Email, emma.scotter@auckland.ac.nz; Telephone, +64 9 923 1350

Acknowledgements and funding

This publication is dedicated to the incredible patients and families who contribute to our research. We thank Marika Eszes at the Centre for Brain Research, University of Auckland, New Zealand; Nailah Siddique at the Northwestern University Feinberg School of Medicine, Chicago, USA; Sashika Selvaduncko and Claire Troakes at the London Neurodegenerative Diseases Brain Bank and Brains for Dementia; and the Neurological Foundation of New Zealand for their ongoing financial support of the Human Brain Bank. We also thank Fairlie Hinton and Dr. Catriona McLean at the Victorian Brain Bank, which is supported by The Florey Institute of Neuroscience and Mental Health, The Alfred and the Victorian Forensic Institute of Medicine and funded in part by Parkinson's Victoria, MND Victoria, FightMND and Yulgilbar Foundation. The imaging data reported in this paper were obtained at the Biomedical Imaging Research Unit (BIRU), operated by the Faculty of Medical and Health Sciences' Technical Services at the University of Auckland. KT was funded by a doctoral scholarship from Amelia Pais-Rodriguez and Marcus Gerbich. BVD and MD were funded by the Michael J Fox Foundation [Grant ID: 16420]. BVD was also funded by a Health Research Council Sir Charles Hercus Health Research Fellowship [21/034]. ELS was supported by Marsden FastStart and Rutherford Discovery Fellowship funding from the Royal Society of New Zealand [15-UOA-157, 15-UOA-003]. This work was also supported by grants from Motor Neuron Disease NZ, Freemasons Foundation of New Zealand, Matteo de Nora, Sir Thomas and Lady Duncan Trust and the Coker Family Trust (to MD), and PaR NZ Golfing. No funding body played any role in the design of the study, nor in the collection, analysis, or interpretation of data nor in writing the manuscript.

Authors' contributions

KMT, BVD, HCM, MEVS, JHY, NFM conducted or designed experiments; KMT, BVD, HCM, MEVS, ELS performed data analysis or designed analysis methods; CT conducted neuropathological diagnostics; MD provided study supervision and resourcing; RLMF, MAC, TS, CES coordinated the banking and use of human tissue for study; TS, CES, GAN identified the *UBQLN2* patients; KLW, LH performed relatedness analysis; KMT, BVD,

ELS wrote the manuscript; GAN, ELS conceived of the study. ELS designed the study. All authors read, edited, and approved the final manuscript.

Abstract

Mutations in the *UBQLN2* gene cause X-linked dominant amyotrophic lateral sclerosis (ALS) and/or frontotemporal dementia (FTD) characterised by ubiquilin 2 aggregates in neurons of the motor cortex, hippocampus, cerebellum, and spinal cord. However, ubiquilin 2 neuropathology is also seen in sporadic and familial ALS or FTD cases not caused by *UBQLN2* mutations, particularly *C9ORF72*-linked cases. This makes the mechanistic role of ubiquilin 2 mutations and the value of ubiquilin 2 pathology for predicting genotype unclear. Here we examine a cohort of 31 genotypically diverse ALS cases with or without FTD, including four cases with *UBQLN2* mutations (resulting in p.P497H, p.P506S, and two cases with p.T487I). Using double-, triple-, and five-label fluorescent immunohistochemistry, we mapped the co-localisation of ubiquilin 2 with phosphorylated TDP-43 (pTDP-43), dipeptide repeat aggregates, and p62, in the hippocampus of controls (n=5), or ALS with or without FTD in sporadic (n=19), unknown familial (n=3), *SOD1*-linked (n=1), *C9ORF72*-linked (n=4), and *UBQLN2*-linked (n=4) cases. We differentiate between i) ubiquilin 2 aggregation together with, or driven by, pTDP-43 or dipeptide repeat proteins, and ii) ubiquilin 2 self-aggregation driven by *UBQLN2* gene mutations. Together we describe a hippocampal protein aggregation signature that fully distinguishes mutant from wildtype ubiquilin 2 in ALS with or without FTD, whereby mutant ubiquilin 2 is more prone than wildtype to aggregate independently of driving factors. This neuropathological signature can be used to assess the pathogenicity of *UBQLN2* gene mutations and to understand the mechanisms of *UBQLN2*-linked disease.

Keywords: *UBQLN2*, ubiquilin 2, amyotrophic lateral sclerosis (ALS), frontotemporal dementia (FTD), neuropathology, hippocampus, human, TDP-43, polyGP, polyGA

Introduction

UBQLN2 gene mutations are a rare cause of amyotrophic lateral sclerosis (ALS) with or without dementia, and the only known causal mutations on the X-chromosome. *UBQLN2* [NM_013444] encodes the ubiquilin 2 protein, the best studied of five human ubiquilins, which contains a unique PXX domain comprising 12 proline-rich tandem repeats [1,2]. Like other ALS- and FTD-linked degradation proteins (sequestosome 1/p62 (hereafter p62), valosin-containing protein, optineurin, and TANK-binding kinase 1), a key role for ubiquilin 2 is to bind ubiquitinated, misfolded, and aggregated protein cargos, triaging them between the proteasome and autophagy intracellular degradation pathways [3–6]. New evidence suggests that ubiquilin 2 also undergoes reversible liquid-liquid phase separation, allowing it to bind ubiquitin-labelled proteins within phase-separated stress granules. Upon ubiquitinated protein binding, ubiquilin 2 falls out of the liquid-droplet phase, plucking its cargo from the stress granule for delivery to the proteasome; ubiquilin 2 is therefore also implicated in stress granule disassembly [7–10].

These roles at the interface between RNA processing and protein degradation — two key pathways in ALS and FTD pathogenesis — underpin why ubiquilin 2 mutations cause disease. ALS and/or FTD (ALS/FTD)-causing *UBQLN2* mutations that alter residues flanking and within the PXX domain impair ubiquilin 2 binding to the proteasome, and promote self-oligomerisation and liquid-to-solid rather than liquid-liquid phase transition [9,11–14]. The mutation c.1490C>A, resulting in p.P497H, was the first disease-causing *UBQLN2* mutation identified, leading to the discovery in unrelated ALS/FTD families of mutations c.1489C>T (p.P497S), c.1516C>A (p.P506T), c.1525C>T (p.P509S) and c.1573C>T (p.P525S) all altering the PXX domain [1]. A c.1516C>T mutation, resulting in p.P506S also within the PXX domain, was later identified in a family with young onset ALS, ALS with FTD onset, or pure spastic paraplegia [15] while a c.1460C>T mutation, resulting in p.T487I just upstream of the PXX region, was found in two families with members in New Zealand and Australia [16,17]. *UBQLN2* mutations/variants have also been identified in ALS/FTD cases altering other residues within or flanking the PXX domain; in the ubiquitin-like domain; the stress-induced protein 1-like domains; or outside of known domains [18–37]. However, it is currently uncertain whether all of these

UBQLN2 variants are pathogenic (disease-causing).

The neuropathology of ALS/FTD caused by pathogenic *UBQLN2* mutations is characterised by aggregated ubiquilin 2 in the motor cortex, spinal cord, cerebellum, and hippocampus [1,15,17,23,38]. We previously reported ubiquilin 2-positive aggregates in the hippocampus of an individual with p.T487I *UBQLN2*-linked ALS+FTD, but not in sporadic ALS [38]. However, ubiquilin 2 inclusions are not specific to *UBQLN2*-linked ALS/FTD cases and have been identified previously in sporadic and familial ALS, and ALS-dementia, regardless of whether ubiquilin 2 is wildtype or mutant [1,15,17,23,38,39]. Some of these ubiquilin 2 inclusions are immunopositive for other ALS/FTD-linked proteins such as pan-TDP-43 or phosphorylated TDP-43 (pTDP-43), FUS, p62, optineurin, or ubiquitin [1,17,40–44]. In addition, deposition of ubiquilin 2 in the hippocampus is a characteristic feature of ALS/FTD caused by *C9ORF72* hexanucleotide repeat expansions, in which ubiquilin 2 is seen in the presence of dipeptide repeat (DPR) proteins [39]. Thus, while ubiquilin 2 is clearly involved in ALS/FTD pathogenesis regardless of aetiology, the role of *UBQLN2* mutations and the predictive value of ubiquilin 2 labelling in relation to genotype is still unclear.

There is a clear need to determine whether *UBQLN2* mutations cause ubiquilin 2 neuropathology that is distinct from the wildtype ubiquilin 2 neuropathology that is seen in ALS/FTD with other genotypes. If they do, then defining a pathological signature for *UBQLN2*-linked disease will provide mechanistic insights and aid assessment of the pathogenicity of *UBQLN2* genetic variants which are not yet confirmed to be causative. Because ubiquilin 2 aggregation across a range of ALS/FTD genotypes occurs in the hippocampus, this region may provide insight into the requirements for mutant and wildtype ubiquilin 2 aggregation. Here we map the hippocampal ubiquilin 2 protein deposition signature with respect to pTDP-43, two *C9ORF72*-linked DPR proteins, and p62, in ALS/FTD with and without *UBQLN2* mutation.

Materials and methods

Systematic review of *UBQLN2*-linked ALS/FTD neuropathology

Journal articles were identified using PubMed that were published between Jan 1993 and September 2021. Search terms were *UBQLN2*, ubiquilin 2, amyotrophic lateral sclerosis, and ALS, combined with neuropathology, tissue, or immunohistochemistry. Articles which did not contain ubiquilin 2 neuropathological information in post-mortem ALS/FTD human brain tissue, were not primary research articles, or were not published in English were excluded. Seven papers were identified from which neuropathological data for TDP-43, ubiquilin 2, ubiquitin, p62, *C9ORF72*-linked DPR proteins, FUS, and SOD1 protein aggregates in the spinal cord and hippocampus were extracted and tabulated.

Patient demographics and hippocampal brain tissue

Formalin-fixed paraffin-embedded (FFPE) post-mortem brain tissue from 5 neurologically normal and 28 ALS cases with or without FTD, processed as previously described [45] were obtained from the Neurological Foundation Human Brain Bank at the Centre for Brain Research, Auckland, New Zealand. Patient demographic and clinical information is summarised in Table S1. These included nineteen cases with sporadic ALS (one of whom had co-morbid FTD), three with familial ALS of unknown genotype, one with *SOD1*-linked ALS (p.E101G), four with *C9ORF72*-linked ALS, and one with ALS+FTD with the *UBQLN2* p.T487I mutation (pedigree ID FALS5 IV:18 in Fig. 1A of [17] and in this report; and coded MN17 in Figure 1D of [38] and in this report). It should be noted that the latter (MN17/ FALS5 IV:18) was stored in fixative for 7 years before embedding. All non-*SOD1*-linked NZ cases had confirmed pTDP-43 proteinopathy in the motor cortex. FFPE hippocampal tissue was also obtained from the Victoria Brain Bank from an affected family member of the *UBQLN2* p.T487I case, who had ALS+FTD and was also positive for the mutation (pedigree ID V:7 in Figure 1A of [17] and in this report); and from two unrelated *UBQLN2*-linked cases from the London Neurodegenerative Diseases Brain Bank and Brains for Dementia (p.P506S (ALS+FTD), pedigree ID II.2 in Fig. 1B of [15]), and the Northwestern University Feinberg School of Medicine, USA (p.P497H (ALS), pedigree ID V:I of Family #186 in Fig. 1A of [1]). All clinical and neuropathological diagnoses were conducted as described previously [1,15,17,38].

Double-, triple-, and five-label fluorescent immunohistochemistry

Fluorescence immunohistochemistry was performed as described previously [46,47]. Briefly, tissue sections were cut with a microtome in the transverse plane at a thickness of 7-10 µm and mounted onto Superfrost Plus slides (Thermo Fisher Scientific). Mounted sections were dried at room temperature for a minimum of 1 week before immunohistochemistry. Slides were heated to 60 °C for 1 h on a hot plate, then dewaxed and rehydrated through a xylene-alcohol-water series: 100% xylene, 2x 30 min; 100% ethanol, 2x 15 min; 95%, 85%, 75% ethanol, 5 min each; water 3x 5 min. Antigens were retrieved through immersion in 10 mM sodium citrate buffer (0.05% Tween 20, pH 6.0) in a pressure cooker (Retriever 2100, Electron Microscopy Sciences) at 120 °C for 20 min and cooled to room temperature for 100 min. Sections were washed 3x 5 min in 1x phosphate-buffered saline (PBS) and wax borders were drawn with an ImmEdge Hydrophobic Barrier PAP pen. Sections were permeabilised in PBS-T (PBS with 0.2% Triton™ X100) for 15 min at 4 °C, followed by 3x 5-min PBS washes. Lipofuscin autofluorescence was quenched using TrueBlack® Lipofuscin quencher (Biotium) 1:20 in 70% ethanol for at least 30 seconds followed by three vigorous water washes. Sections were blocked with 10% normal goat or donkey serum (Thermo Fisher Scientific) in PBS for 1 h, then incubated at 4 °C overnight with primary antibodies (Table S2). Following PBS washes, species- and isotype-specific secondary antibodies and Hoechst 33342 nuclear stain (Table S2) were applied for 3 h in 1% normal goat or donkey serum at room temperature. After final 3x 5-min PBS washes, sections were coverslipped with #1.5 coverslips (Menzel-Gläser) using ProLong® Gold Antifade Mountant (Thermo Fisher Scientific). Neurologically normal control samples, bleed-through, secondaries-only, and cross-reactivity control sections were included for each staining (Figs. S2, S3, S4, S5, S6, S7, S8).

Image acquisition

Wide-field double- and triple-label images were acquired using a Nikon Eclipse N*i*-E microscope (20x magnification, 0.50 NA) with a Nikon DS-Ri2 camera using NIS elements (Nikon, version 4.20). Sections were imaged with the same exposure time and gain settings for each staining combination where possible. *UBQLN2*-linked ALS+FTD

212 case V:7-p.T487I showed consistently poor Hoechst immunoreactivity, while *UBQLN2*-
213 linked ALS+FTD case MN17-p.T487I showed poor immunoreactivity overall, likely due
214 to long-term fixation, therefore a longer exposure was used for both cases when imaging.
215
216 Multiplex (five-label) images were acquired using a Zeiss Z2 Axioimager with a
217 MetaSystems VSlide slide scanning microscope (20x dry magnification lens, 0.9 NA) with
218 a Colibri 7 solid-state fluorescent light source. Single filters, as described and validated
219 previously [48], were used to excite fluorophores and detect the following wavelengths:
220 Filter set #1 (LED 385; Em 447/60 nm), #3 (LED 475; Em 527/20 nm), #4 (LED 555; Em
221 580/23 nm), #5 (LED 590; Em 628/32 nm), #6 (LED 630; Em 676/29 nm), and #7 (LED
222 735; Em 809/81 nm) and visualised with MetaFer software (MetaSystems, v.3.12.1)
223 equipped with a CoolCube 4m TEC (monochrome) sCMOS digital camera. Image tiles
224 were seamlessly stitched using MetaCyte software, and stitched images were extracted
225 using VSViewer software (MetaSystems, v.1.1.106).
226
227 Stimulated emission depletion (STED) images were acquired using an Abberior Facility
228 STED microscope (60x UPLXAPO oil immersion lens, 1.42 NA) using ImSpector
229 Lightbox software (Specim, v.16.3.13779). A 561-nm pulsed diode laser was used to
230 excite Alexa Fluor 594, and a 640-nm diode laser was used to excite Alexa Fluor 647. For
231 STED imaging, a pulsed 775-nm laser was used for depletion of both fluorophores. After
232 scanning, the images were processed using the PureDenoise plugin [49] for ImageJ
233 (National Institutes of Health, USA v1.53f51).
234
235 Confocal images of triple-label immunohistochemically stained tissue were acquired using
236 a Zeiss LSM 800 Airyscan confocal laser scanning microscope (63x magnification oil
237 immersion lens, 1.4 NA, Z-step 0.25 µm) with ZEN software (Carl Zeiss, ZEN 3.1 Blue
238 Edition). Maximum intensity Z-projections and orthogonal projections were generated and
239 processed using ZEN 3.1 software.
240
241 Final figures were composed using Adobe Photoshop CC (Adobe Systems Incorporated,
242 v20.0.6).

Relatedness analysis

To further examine the p.T487I mutation in ALS/FTD, genome-wide genotype data from the family of *UBQLN2*-linked ALS+FTD case MN17 (FALS5) and another Australian family with an identical p.T487I mutation (FALS14) were analysed to determine whether they inherited the mutation from a common ancestor (pedigree in Fig. S1, sample information in Table S3). These two families were previously reported to share a haplotype identical-by-state over the *UBQLN2* locus [17], but genealogy analysis had been unable to link the pedigrees. Three individuals from FALS5 (all affected, pedigree IDs III:8, IV:9, IV:18 (MN17)) and two individuals from FALS14 (pedigree IDs II:1 (unaffected) and III:2 (affected)) underwent SNP genotyping using the Illumina Infinium Global Screening Array v2.0. Identity-by-descent (IBD) analysis was performed using XIBD software [50] with the combined HapMap Phase II and III European (CEU) cohort as a reference dataset. SNPs in high linkage disequilibrium ($r^2 > 0.95$) or SNPs with a low minor allele frequency (MAF < 0.01) were removed from analysis, as well as SNPs with missing genotype calls in two or more samples. 39,002 SNPs remained for analysis and 211 IBD segments greater than 3 cM were identified. The degree of relationship was estimated for each pair of samples using the lengths of inferred IBD segments as in Estimation of Recent Shared Ancestry [51].

Results

Ubiquilin 2 labelling in previous studies fails to discriminate between *UBQLN2*-linked and other genotypes of ALS/FTD

Systematic review of the literature describing ubiquilin 2 neuropathology in human ALS/FTD identified 137 results, of which 7 articles met the criteria for full review. The neuropathology of ubiquilin 2 with respect to six other ALS/FTD-linked proteins in specific CNS regions is summarised in Fig. 1. Ubiquilin 2 neuropathology in the spinal cord is present in ALS/FTD cases with *UBQLN2* mutations, but is also frequently found aggregating in sporadic ALS cases and in ALS/FTD with other genotypes where it presumably co-localises with aggregates of pTDP-43 and/or mutant proteins. Ubiquilin 2 neuropathology in the hippocampal molecular layer was most frequently reported upon, being found in *UBQLN2*-linked and *C9ORF72*-linked ALS/FTD. Ubiquilin 2

neuropathology in the hippocampal granule cell layer was inconsistent between cases of *UBQLN2*-linked ALS/FTD but was found in all cases of *C9ORF72*-linked ALS/FTD and therefore also in "ALS-dementia" ([1], later confirmed to be *C9ORF72*-positive) and in a single sporadic ALS/FTD case. Overall, neither ubiquilin 2 staining alone nor in combinations previously tested could distinguish mutant ubiquilin 2 aggregation in *UBQLN2*-linked ALS/FTD from wildtype ubiquilin 2 aggregation in other ALS/FTD genotypes.

Ubiquilin 2 and pTDP-43 protein pathology

Sporadic ALS: No cases showed hippocampal ubiquilin 2, but certain cases had hippocampal pTDP-43

No hippocampal ubiquilin 2 pathology was observed in any sporadic ALS case. Of the 19 sporadic ALS cases examined (one of which had co-morbid FTD), 6 cases (32%; including the case with FTD), had perinuclear pTDP-43-positive neuronal cytoplasmic inclusions (NCIs) in the granule cells of the dentate gyrus but not the molecular layer. These ranged in density from sparse to frequent, suggestive of stage 4 pTDP-43 proteinopathy [52], and were always ubiquilin 2-negative (Fig. 2A1-F1, white arrowheads). The remaining 13 sporadic ALS cases (68%) were devoid of either ubiquilin 2 or pTDP-43 in both the granule cell and molecular layers of the hippocampus (Fig. S2). Similarly, no ubiquilin 2 or pTDP-43 aggregates were observed in 5 controls, 3 familial ALS cases of unknown aetiology (unrelated to one another; MN11, MN14, and MN21), or a *SOD1*-linked ALS case (MN24, p.E101G), nor when primary antibodies were omitted (Fig. S2).

UBQLN2-linked ALS/FTD: All cases showed hippocampal molecular layer ubiquilin 2, some also had hippocampal granule cell layer pTDP-43

All *UBQLN2*-linked ALS/FTD cases had ubiquilin 2-positive but pTDP-43-negative punctate aggregates in the hippocampal molecular layer, albeit at variable loads (Fig. 2G-J, green arrowheads). They appeared to be localised to the dendritic spines of the hippocampal granule cells, as reported previously in *UBQLN2*-linked ALS/FTD and in mutant *UBQLN2* rodent models [1,53]. Only ALS+FTD case V:7 carrying the *UBQLN2*

p.T487I mutation showed pTDP-43 co-localisation with this molecular layer ubiquilin 2, and this was only in a single aggregate (Fig. 2I, white arrow in main image).

In the granule cell layer, one *UBQLN2* p.P497H case (Fig. 2G) and one *UBQLN2* p.T487I case (MN17, Fig. 2H) were devoid of ubiquilin 2 and pTDP-43 aggregates, consistent with previous findings [1,38]. In contrast, *UBQLN2* p.T487I case V:7 showed very sparse pTDP-43-positive cytoplasmic aggregates in the granule cell layer that were negative for ubiquilin 2 (Fig. 2I2, white arrowhead). In further contrast, and consistent with Gkazi and colleagues [15], a *UBQLN2* p.P506S case had abundant pTDP-43-positive cytoplasmic aggregates in the granule cell layer, that either co-localised with ubiquilin 2 (Fig. 2J1, unfilled green arrowheads) or were independent of ubiquilin 2 (Fig. 2J and J3, white arrowheads). Importantly, while punctate ubiquilin 2 aggregates in the molecular layer dendrites in all *UBQLN2*-linked ALS/FTD cases were independent of pTDP-43, the larger ubiquilin 2 aggregates in the granule cell layer somata in the p.P506S case were always co-localised with pTDP-43. Mutant ubiquilin 2 aggregation in the granule cell layer was therefore likely scaffolded or 'seeded' by pTDP-43, but aggregation in the molecular layer was independent of a known scaffold.

C9ORF72-linked ALS: All cases showed hippocampal molecular layer and granule cell layer ubiquilin 2, some also had hippocampal granule cell layer pTDP-43

C9ORF72-linked ALS/FTD cases are known to be positive in the hippocampus for aggregates of both ubiquilin 2 [39,54] and dipeptide repeat (DPR) proteins translated from the expanded repeat [55,56]. *C9ORF72*-positive ALS cases MN2, MN18, and MN23 showed numerous punctate dendritic ubiquilin 2 aggregates and ubiquilin 2-positive dystrophic neurites in the molecular layer (Fig. 2K1-M1, green arrowheads), and compact, star-shaped ubiquilin 2 aggregates in the granule cell layer cell bodies (Fig. 2K2-M2, green arrowheads). These *C9ORF72* cases were devoid of hippocampal pTDP-43. In contrast, *C9ORF72*-positive case MN28 had similar granule cell and molecular layer ubiquilin 2 aggregates (Fig. 2N1-3, green arrowheads), but with additional pTDP-43 aggregates in the granule cell layer that co-localised very rarely with ubiquilin 2 (Fig. 2N1, unfilled green arrowhead) or were independent of ubiquilin 2 (Fig. 2N3, white arrowheads). Overall, in

all *C9ORF72*-linked ALS cases both punctate ubiquilin 2 aggregates in the molecular layer dendrites and the majority of 'starburst' ubiquilin 2 aggregates in the granule cell layer somata were independent of pTDP-43. Wildtype ubiquilin 2 was therefore not 'seeded' to aggregate in the granule cell layer by pTDP-43, and aggregated in the molecular layer independently of a known scaffold.

Ubiquilin 2 and DPR protein pathology

UBQLN2-linked ALS/FTD: DPR proteins were not components of hippocampal ubiquilin 2 pathology

As expected, all four *UBQLN2*-linked ALS/FTD cases were devoid of poly(glycine-arginine) (polyGA) and poly(glycine-proline) (polyGP) DPR aggregates (Fig. 3A-D), thus DPR proteins were not co-localised with the ubiquilin 2 detected in the molecular layer of all four cases (Fig. 3A1-D1, green arrowheads), nor were DPR proteins co-localised with the ubiquilin 2 (and therefore pTDP-43) in the granule cell layer of *UBQLN2*-linked case p.P506S (Fig. 3D2, green arrowhead).

C9ORF72-linked ALS: PolyGP and polyGA DPR aggregates were requisite components of ubiquilin 2 pathology

The abundant punctate and skein-like ubiquilin 2 aggregates in the molecular layer dendrites of *C9ORF72*-linked ALS cases, as described in Fig. 2, were all polyGA- and polyGP-negative (Fig. 3E1-H1", green arrowheads). However, as reported previously, all *C9ORF72*-linked cases had polyGA and/or polyGP aggregates in the granule cell layer somata (Fig. 3E2-H2"). PolyGP aggregates were rare in all cases and virtually always co-localised with polyGA (Fig. 3E2 & H2, pink arrowheads). PolyGA aggregates were often (Fig. 3E2-H2, yellow arrowheads) but not always (Fig. 3E2-H2, red and pink arrowheads) co-localised with ubiquilin 2.

Although these granule cell layer DPR aggregates were sometimes devoid of ubiquilin 2 co-labelling, the converse was not observed. Granule cell layer ubiquilin 2 aggregates always co-localised with DPR aggregates; ubiquilin 2 aggregates were never independent of DPR proteins (Fig. 3E2-H2, yellow arrowheads [1,38,39]). Even *C9ORF72*-positive

case MN28 (Fig. 3H), which had granule cell layer pTDP-43 aggregates, showed granule cell layer ubiquilin 2 that always co-localised with DPR aggregates. Further investigation in this case demonstrated that 1-2 cells per section of the dentate gyrus granule cell layer contained a DPR aggregate that was surrounded by a pTDP-43 'shell', either with polyGA, polyGP, and ubiquilin 2 co-localisation (Fig. S8A) or with polyGA and polyGP but without ubiquilin 2 (Fig. S8B). This supports a previous report that ubiquilin 2 in *C9ORF72*-linked cases rarely co-localises with granule cell layer pTDP-43, and if so, only when DPRs are also present in the aggregate [57]. Therefore, wildtype ubiquilin 2 aggregation was likely 'seeded' in the granule cell layer by polyGA, but not by pTDP-43.

Ubiquilin 2 and p62 protein pathology

UBQLN2-linked ALS/FTD versus C9ORF72-linked ALS: Only mutant ubiquilin 2 aggregates in the hippocampal molecular layer were p62 positive

Like ubiquilin 2, p62 is a ubiquitin-binding protein which acts as a cargo adaptor for both the ubiquitin-proteasome system and autophagy and is linked aetiologically to ALS [58–61]. We sought to investigate whether the ubiquilin 2 aggregates identified in the molecular layer dendrites in both *UBQLN2*-linked and *C9ORF72*-linked cases were p62 positive. In the four *UBQLN2*-linked ALS/FTD cases, the mutant ubiquilin 2 aggregates in the molecular layer co-localised with p62 (Fig. 4A-D, orange arrowheads). Only very occasionally were ubiquilin 2 aggregates in this region found to be p62 negative (Fig. 4A-D, green arrowheads). In contrast, in *C9ORF72*-linked ALS cases the wildtype ubiquilin 2 aggregates in the molecular layer only very rarely co-localised with p62 (Fig. 4E, orange arrowheads) and were predominantly p62 negative. Therefore, mutant but not wildtype ubiquilin 2 promotes or scaffolds the co-aggregation of p62.

To further clarify the extent to which ubiquilin 2 aggregates were p62 labelled in *UBQLN2*- and *C9ORF72*-linked cases, we performed confocal microscopy of molecular layer aggregates in two cases with representative molecular layer ubiquilin 2 pathology (*UBQLN2* p.P506S, and *C9ORF72*-positive MN28). This confirmed that mutant ubiquilin 2 aggregates in the molecular layer in *UBQLN2*-linked ALS/FTD were almost all co-localised with p62 (Fig. 4F), while wildtype ubiquilin 2 aggregates in the molecular layer

in *C9ORF72*-linked ALS were very rarely p62 positive (Fig. 4G). Further, the mutant ubiquilin 2 aggregates were morphologically distinct from wildtype; mutant ubiquilin 2 formed small compact aggregates (Fig. 4F) while wildtype ubiquilin 2 formed both small compact aggregates *and* wispy skein-like structures (Fig. 4G).

Combined neuropathological signatures discriminate between *UBQLN2*-linked, *C9ORF72*-linked, sporadic, and unknown familial cases

Integration of all neuropathological findings (Fig. 5) revealed a characteristic hippocampal neuropathological signature for *UBQLN2*-linked ALS/FTD, which was distinct from that in other forms of ALS/FTD.

Sporadic ALS cases were wholly devoid of hippocampal ubiquilin 2 or DPR protein pathology, with a minority of cases showing pTDP-43 aggregates in the granule cells that were ubiquilin 2 negative. Thus, wildtype ubiquilin 2 is not seeded/ scaffolded to aggregate by pTDP-43 aggregation.

Ubiquilin 2 hippocampal pathology was present in both *UBQLN2*-linked ALS/FTD and *C9ORF72*-linked ALS, but these genotypes could be discriminated when ubiquilin 2 was co-labelled with pTDP-43, DPR proteins, or p62. *C9ORF72*-linked cases always showed granule cell layer ubiquilin 2 that co-localised with DPR aggregates, but rarely pTDP-43. This supports the lack of seeding of wildtype ubiquilin 2 aggregation by pTDP-43, but suggests that wildtype ubiquilin 2 can be seeded by polyGA. In contrast, *UBQLN2*-linked cases showed granule cell layer ubiquilin 2 if co-localised pTDP-43 was present. Therefore, mutant ubiquilin 2 is more aggregation-prone than wildtype, being seeded by pTDP-43.

In addition, *C9ORF72*-linked cases showed molecular layer ubiquilin 2 that was wispy or punctate and predominantly p62 negative, while *UBQLN2*-linked cases showed molecular layer ubiquilin 2 that was punctate and always p62 positive. Mutant but not wildtype ubiquilin 2 aggregates thus promote the co-aggregation of p62, and this may relate to their

conformational differences. Overall, mutant ubiquilin 2 causes unique neuropathology that is shared by p.P506S, p.P497H, and p.T487I ubiquilin 2 (Fig. 6).

UBQLN2 p.T487I mutation in ALS/FTD families FALS5 and FALS14 was inherited from a common ancestor

Since the initial report by Williams et al. [17] of an identical *UBQLN2* p.T487I mutation in ALS families FALS5 and FALS14, we report here that cases MN17 (IV:18) and V:7 from family FALS5 developed ALS+FTD, indicating that FTD is part of the clinical phenotype in that family. To further examine relatedness between the families and confirm that the *UBQLN2* p.T487I mutation arose in a common founder, we performed identity-by-descent (IBD) analysis. IBD segments were identified over the *UBQLN2* locus between all four affected individuals from both families (Table 1), while there were no IBD segments inferred over *UBQLN2* between the affected individuals from FALS5 and the unaffected individual from FALS14 who did not carry the *UBQLN2* p.T487I mutation. The interval shared by all four affected individuals spanned rs952836 to rs6423133 and is 68 cM in length. This confirms a founder effect of *UBQLN2* p.T487I in FALS5 and FALS14. The genotyped individuals across these families are estimated to be 4th- to 5th-degree relatives (1st cousins once removed - 2nd cousins) (Table 2), now confirming segregation of the *UBQLN2* p.T487I mutation in 17 individuals from the proposed combined Australia-New Zealand pedigree and providing further strong genetic evidence, in addition to the neuropathological evidence, that *UBQLN2* p.T487I is pathogenic for ALS/FTD.

Discussion

ALS shows considerable clinical, pathological, and genetic heterogeneity [62–64]. While TDP-43 proteinopathy is seen in 97% of cases [40,43,65], ALS/FTD-causing genetic mutations can cause deposition of the encoded mutant protein leading to additional pathological aggregate signatures. We previously exploited this to infer *C9ORF72* repeat expansion genotypes [56,66] through neuropathological screening of our New Zealand ALS cases [38]. Mutant *SOD1* [67,68], *FUS* [44], and certain other genotypes [69,70] can also be inferred from neuropathology. However, for many ALS/FTD genes — particularly those such as *TARDBP*, *SQSTM1*, and *UBQLN2* that encode proteins already within the hallmark TDP-43 inclusions — no completely discriminating neuropathology has been

reported [42,69,71–75]. This has hampered the validation of pathogenicity of novel variants in these genes, in turn obscuring understanding of protein domains and molecular processes important to ALS/FTD pathogenesis. However, we report here a unique neuropathological signature for mutant ubiquilin 2 in the hippocampus that discriminates *UBQLN2*-linked ALS/FTD cases from all others tested.

pTDP-43 in *UBQLN2*-linked cases: An independent pathology

Before discussing the unique pattern of hippocampal ubiquilin 2 pathology shared by *UBQLN2*-linked cases, it must first be noted that pTDP-43 deposition was variable. Two of the four *UBQLN2*-linked cases were devoid of granule cell layer pTDP-43 aggregates (p.P497H (ALS) and MN17-p.T487I (ALS+FTD)), one case had very sparse granule cell layer pTDP-43 aggregates that were ubiquilin 2-negative (V:7-p.T487I (ALS+FTD)), and one case showed frequent granule cell layer pTDP-43 aggregates that were mostly ubiquilin 2-positive (p.P506S (ALS+FTD)). Although pTDP-43 aggregates are nearly ubiquitous in the ALS spinal cord and motor cortex, only in ~15-30% of ALS cases are they found in the hippocampus [52,76]. Our findings suggest that sequential pTDP-43 deposition occurs in the context of *UBQLN2*-linked ALS/FTD just as it does in sporadic and *C9ORF72*-linked ALS/FTD.

Because pTDP-43 deposition correlates regionally with neurodegeneration, including in the hippocampus [39,52,57,77], hippocampal pTDP-43 has been proposed to promote hippocampal cell loss and the development of FTD [39]. Indeed, pTDP-43 is seen in the hippocampus in 80-100% of behavioural variant FTD (bvFTD) cases compared to only 15-30% of ALS cases [76,77]. The sequential regional deposition of pTDP-43 in bvFTD occurs in almost the reverse direction to that in ALS, with severe pTDP-43 pathology progressing from the orbitofrontal regions and rhinal cortex, via the hippocampus and anterior cingulate cortex to the motor cortex and spinal cord [76,77]. Therefore, ALS cases that also manifest with FTD are highly likely to have pTDP-43 in the anterior cingulate and hippocampus [76].

Indeed, three of the four cases with FTD in our study cohort (75%) showed hippocampal granule cell layer pTDP-43 aggregates. These were the *UBQLN2* p.P506S case (initial presentation of FTD progressing to ALS), *UBQLN2*-linked case V:7-p.T487I (complex neuropsychiatric history prior to diagnosis of ALS with personality and behavioural changes), and sporadic case MN15 (initial presentation of FTD progressing to ALS). Also fitting this paradigm, the *UBQLN2* p.P497H case did not have FTD and was devoid of granule cell layer pTDP-43 aggregates. The exception to this pattern in ALS+FTD was *UBQLN2*-linked case MN17-p.T487I in which initial presentation was ALS, yet despite later manifesting FTD did not have granule cell layer pTDP-43 aggregates. Conversely, five of the six sporadic ALS cases with hippocampal pTDP-43, and *C9ORF72*-linked case MN28 with hippocampal pTDP-43, had no clinical history of FTD. Therefore, while FTD cases frequently have hippocampal granule cell layer TDP-43, the converse is not true, such that having hippocampal pTDP-43 does not necessarily predict FTD phenotype.

UBQLN2 and *C9ORF72* mutations are more likely than other genes to cause mixed ALS/FTD phenotypes [1,32,36,63,65,78–81] so hippocampal deposition of ubiquilin 2 may further promote FTD phenotype.

Wildtype ubiquilin 2 pathology in *C9ORF72*-linked cases

Hippocampal ubiquilin 2 deposition is a known and striking feature of *C9ORF72*-linked ALS/FTD [39]. In our *C9ORF72*-linked ALS cases, large stellate granule cell layer ubiquilin 2 was found to preferentially co-localise with the aggregation-prone polyGA DPR protein compared to polyGP. Furthermore, polyGP aggregates were very rarely independent of polyGA. These findings support the emerging consensus that polyGA aggregates 'seed' polyGP protein aggregation [82–84]. Similar observations were made by Mackenzie and colleagues [57] of aggregates with a core of polyGA surrounded by an aggregated TDP-43 shell; a finding recapitulated here and supported by *in vitro* work showing polyGA aggregation preceding TDP-43 accumulation [85]. The ability of DPR proteins to seed ubiquilin 2 however, appears more complex. We previously showed ubiquilin 2 at the core of polyGP-positive aggregates, but we did not co-label for polyGA [38]. STED imaging in the current study shows that ubiquilin 2 may either surround

polyGA or be enmeshed with it, suggesting that in *C9ORF72*-linked ALS pathogenesis, the interaction between aggregating polyGA and ubiquilin 2 may be an early event.

In contrast to ubiquilin 2 co-aggregation with large stellate DPR proteins in the granule cell layer, small neuritic ubiquilin 2 aggregates in *C9ORF72*-linked cases punctuated the molecular layer seemingly independent of a nucleating protein. The neurites in which these small aggregates are found likely derive from the granule cells themselves [86,87], so DPR protein inclusions in the somata may promote the aggregation of ubiquilin 2 in the dendrites of the same cell. DPR aggregates can sequester proteasome components [88–90], and loss of C9ORF72 protein function in cells expressing the DPR-encoding variant 2 [91] can impair autophagy [92–97], which may underpin wildtype ubiquilin 2 aggregation in the molecular layer in *C9ORF72*-linked cases.

Mutant ubiquilin 2 pathology in *UBQLN2*-linked cases: A neuropathological signature

Even in its wildtype state, ubiquilin 2 intrinsically self-assembles [3] but there is now ample biophysical evidence demonstrating that mutations to ubiquilin 2 confer an increased propensity to oligomerise and undergo aberrant LLPS, forming insoluble aggregates within the cell [8,9,12,98–100]. Here we confirm that mutant ubiquilin 2 in the human hippocampal granule cell dendrites (molecular layer) is more aggregation-prone than wildtype ubiquilin 2, requiring no aggregated protein scaffold or protein aggregation event in the granule cell soma (granule cell layer).

Our study additionally finds that p62 labelling is essential, while pTDP-43 labelling is dispensable, to confirm cases as being *UBQLN2*-linked. P62 co-localises with pTDP-43 aggregates and DPR proteins in ALS/FTD [55,56,101], or with hyperphosphorylated tau in a range of tauopathies [102–104], or with mutant α-synuclein in synucleinopathies [104,105]. Given this promiscuity for substrates, discrimination between mutant and wildtype ubiquilin 2 by p62 suggests that there are structural or biochemical features of mutant ubiquilin 2 that may be specifically druggable.

In addition to mechanistic insights, the mutant ubiquilin 2 neuropathological signature we describe will enable classification of *UBQLN2* variants of uncertain significance. To date, seven missense mutations in *UBQLN2* have been designated by ClinVar as pathogenic or likely pathogenic (resulting in p.M392V, p.Q425R, p.P440L, p.P497H, p.P497L, p.P497S, p.P506T, https://www.ncbi.nlm.nih.gov/clinvar/, [106]). However, 23 other *UBQLN2* missense changes listed in ClinVar are classified as benign or of uncertain significance, including c.1516C>T resulting in p.P506S. Also, although segregation in a large number of family members in the original report supported pathogenicity of *UBQLN2* c.1460C>T (p.T487I), it is not listed in ClinVar, leaving individual diagnostics labs to perform classification for patient reporting. For many rare *UBQLN2* variants, particularly those found in apparent sALS cases, the implications of a positive genetic result for patients have remained unclear. We encourage uptake of this hippocampal ubiquilin 2 neuropathology signature, by other labs or in collaboration with the authors hereof, as a tool to explore *UBQLN2* variant pathogenicity.

Conclusion

Ubiquilin 2 aggregates are seen in the hippocampus of ALS/FTD cases across a range of genotypes. Wildtype ubiquilin 2 is somewhat aggregation-prone; it co-aggregates with polyGA, but not pTDP-43 and it does not promote the co-aggregation of p62. Mutant ubiquilin 2 is more aggregation-prone than wildtype; either co-aggregating with pTDP-43 or aggregating independently of a known scaffold, and in turn promoting the co-aggregation of p62. This hippocampal ubiquilin 2 neuropathology signature demonstrates that ubiquilin 2 aggregation is likely to play a mechanistic role in *C9ORF72*-linked and *UBQLN2*-linked ALS/FTD, and provides a definitive framework for exploring the biological implications of *UBQLN2* genetic variation.

List of abbreviations

ALS	Amyotrophic lateral sclerosis
bvFTD	Behavioural variant FTD
C9ORF72	Chromosome 9 open reading frame 72
DPR	Dipeptide repeat
FFPE	Formalin-fixed paraffin-embedded
FTD	Frontotemporal dementia
IBD	Identity by descent
LLPS	Liquid-liquid phase separation
NCI	Neuronal cytoplasmic inclusions
PBS	Phosphate-buffered saline
PolyGA	Poly(glycine-arginine)
PolyGP	Poly(glycine-proline)
pTDP-43	Phosphorylated TDP-43
SOD1	Superoxide dismutase
STED	Stimulated emission depletion
SQSTM1	Sequestosome 1
TDP-43	Transactive response DNA binding protein 43 kDa

Disclosures and declarations

Data transparency

The datasets used and/or analysed during the current study are available from the corresponding author on reasonable request.

Compliance with ethical standards

Conflicts of interest

The authors declare that they have no conflicts of interest.

Research involving human participants

All protocols were approved by the University of Auckland Human Participants Ethics Committee (New Zealand) and carried out as per approved guidelines. This study was also approved by the Human Research Ethics Committee of Macquarie University (520211013428875).

Informed consent

Informed donor consent and ethical approvals were obtained at each site as described previously [1,15,17,38].

References

1. Deng H-XX, Chen W, Hong S-TT, Boycott KM, Gorrie GH, Siddique N, et al. Mutations in UBQLN2 cause dominant X-linked juvenile and adult-onset ALS and ALS/dementia. Nature. 2011;477(7363):211–5. 10.1038/nature10353
2. Marín I. The ubiquilin gene family: Evolutionary patterns and functional insights. BMC Evolutionary Biology. 2014;14(1):1–22. 10.1186/1471-2148-14-63
3. Hjerpe R, Bett JS, Keuss MJ, Solovyova A, McWilliams TG, Johnson C, et al. UBQLN2 Mediates Autophagy-Independent Protein Aggregate Clearance by the Proteasome. Cell. 2016;166(4):935–49. 10.1016/j.cell.2016.07.001
4. Itakura E, Zavodszky E, Shao S, Wohlever ML, Keenan RJ, Hegde RS. Ubiquilins Chaperone and Triage Mitochondrial Membrane Proteins for Degradation. Molecular Cell. 2016;63(1):21–33. 10.1016/j.molcel.2016.05.020
5. Protter DSW, Parker R. Principles and Properties of Stress Granules. Trends in Cell Biology. 2016;26(9):668–79. 10.1016/j.tcb.2016.05.004
6. Wu JJ, Cai A, Greenslade JE, Higgins NR, Fan C, Le NTT, et al. ALS/FTD mutations in UBQLN2 impede autophagy by reducing autophagosome acidification through loss of function. Proceedings of the National Academy of Sciences. 2020;2(Line 356):201917371.
7. Alexander EJ, Niaki AG, Zhang T, Sarkar J, Liu Y, Nirujogi RS, et al. Ubiquilin 2 modulates ALS/FTD-linked FUS–RNA complex dynamics and stress granule formation. Proceedings of the National Academy of Sciences of the United States of America. 2018;115(49):E11485–94.
8. Dao TP, Kolaitis RM, Kim HJ, O'Donovan K, Martyniak B, Colicino E, et al. Ubiquitin Modulates Liquid-Liquid Phase Separation of UBQLN2 via Disruption of Multivalent Interactions. Molecular Cell. 2018;69(6):965-978.e6.
9. Sharkey LM, Safren N, Pithadia AS, Gerson JE, Dulchavsky M, Fischer S, et al. Mutant UBQLN2 promotes toxicity by modulating intrinsic self-assembly.

Proceedings of the National Academy of Sciences. 2018;115(44):E10495–504. 10.1073/pnas.1810522115

10. Subudhi I, Shorter J. Ubiquilin 2: Shuttling Clients Out of Phase? Molecular Cell. 2018;69(6):919–21. 10.1016/j.molcel.2018.02.030

11. Chang L, Monteiro MJ. Defective proteasome delivery of polyubiquitinated proteins by ubiquilin-2 proteins containing ALS mutations. PLoS ONE. 2015;10(6):1–15. 10.1371/journal.pone.0130162

12. Dao TP, Martyniak B, Canning AJ, Lei Y, Colicino EG, Cosgrove MS, et al. ALS-Linked Mutations Affect UBQLN2 Oligomerization and Phase Separation in a Position- and Amino Acid-Dependent Manner. Structure. 2019;27(6):937-951.e5. 10.1016/j.str.2019.03.012

13. Gilpin KM, Chang L, Monteiro MJ. ALS-linked mutations in ubiquilin-2 or hnRNPA1 reduce interaction between ubiquilin-2 and hnRNPA1. Human Molecular Genetics. 2015;24(9):2565–77. 10.1093/hmg/ddv020

14. Higgins N, Lin B, Monteiro MJ. Lou Gehrig's Disease (ALS): UBQLN2 Mutations Strike Out of Phase. Structure. 2019;27(6):879–81. 10.1016/j.str.2019.05.006

15. Gkazi SA, Troakes C, Topp S, Miller JW, Vance CA, Sreedharan J, et al. Striking phenotypic variation in a family with the P506S UBQLN2 mutation including amyotrophic lateral sclerosis, spastic paraplegia, and frontotemporal dementia. Neurobiology of Aging. 2019;73:229.e5-229.e9. 10.1016/j.neurobiolaging.2018.08.015

16. McCann EP, Williams KL, Fifita JA, Tarr IS, O'Connor J, Rowe DB, et al. The genotype–phenotype landscape of familial amyotrophic lateral sclerosis in Australia. Clinical Genetics. 2017;92(3):259–66. 10.1111/cge.12973

17. Williams KL, Warraich ST, Yang S, Solski JA, Fernando R, Rouleau GA, et al. UBQLN2/ubiquilin 2 mutation and pathology in familial amyotrophic lateral sclerosis. Neurobiology of Aging. 2012;33(10):2527.e3-2527.e10. 10.1016/j.neurobiolaging.2012.05.008

659 18. Chen J, Liu X, Xu Y, Fan D. Association between rare UBQLN2 variants and
660 amyotrophic lateral sclerosis in Chinese population. National Medical Journal
661 of China. 2021;101(12):846–50. 10.3760/cma.j.cn112137-20201015-02835
662 19. Kim HJ, Kwon MJ, Choi WJ, Oh KW, Oh S il, Ki CS, et al. Mutations in
663 UBQLN2 and SIGMAR1 genes are rare in Korean patients with amyotrophic
664 lateral sclerosis. Neurobiology of Aging. 2014;35(8):1957.e7-1957.e8.
665 10.1016/j.neurobiolaging.2014.03.001
666 20. Baglivo M, Manara E, Capodicasa N, Maltese PE, Stuppia L, Michelini S, et
667 al. Early-onset of Frontotemporal Dementia and Amyotrophic Lateral Sclerosis
668 in an Albanian Patient with a c.1319C>T Variant in the UBQLN2 Gene. Open
669 Medicine Journal. 2020;7(1):25–31. 10.2174/1874220302007010025
670 21. Daoud H, Suhail H, Szuto A, Camu W, Salachas F, Meininger V, et al.
671 UBQLN2 mutations are rare in French and French-Canadian amyotrophic
672 lateral sclerosis. Neurobiology of Aging. 2012;33(9):2230.e1-2230.e5.
673 10.1016/j.neurobiolaging.2012.03.015
674 22. Dillen L, van Langenhove T, Engelborghs S, Vandenbulcke M, Sarafov S,
675 Tournev I, et al. Explorative genetic study of UBQLN2 and PFN1 in an
676 extended Flanders-Belgian cohort of frontotemporal lobar degeneration
677 patients. Neurobiology of Aging. 2013;34(6):1711.e1-1711.e5.
678 23. Fahed AC, McDonough B, Gouvion CM, Newell KL, Dure LS, Bebin M, et al.
679 UBQLN2 mutation causing heterogeneous X-linked dominant
680 neurodegeneration. Annals of Neurology. 2014;75(5):793–8.
681 24. Gellera C, Tiloca C, del Bo R, Corrado L, Pensato V, Agostini J, et al. Ubiquilin
682 2 mutations in Italian patients with amyotrophic lateral sclerosis and
683 frontotemporal dementia. Journal of Neurology, Neurosurgery and Psychiatry.
684 2013;84(2):183–7. 10.1136/jnnp-2012-303433
685 25. Huang X, Shen S, Fan D. No evidence for pathogenic role of UBQLN2
686 mutations in sporadic amyotrophic lateral sclerosis in the mainland Chinese
687 population. PLoS ONE. 2017;12(1):1–5. 10.1371/journal.pone.0170943
688 26. Lattante S, le Ber I, Camuzat A, Pariente J, Brice A, Kabashi E. Screening
689 UBQLN-2 in French frontotemporal lobar degeneration and frontotemporal

lobar degeneration-amyotrophic lateral sclerosis patients. Neurobiology of Aging. 2013;34(8):2078.e5-2078.e6. 10.1016/j.neurobiolaging.2013.03.002

27. Luukkainen L, Helisalmi S, Kytövuori L, Ahmasalo R, Solje E, Haapasalo A, et al. Mutation Analysis of the Genes Linked to Early Onset Alzheimer's Disease and Frontotemporal Lobar Degeneration. Journal of Alzheimer's Disease. 2019;69(3):775–82. 10.3233/JAD-181256

28. McLaughlin RL, Kenna KP, Vajda A, Byrne S, Bradley DG, Hardiman O, et al. UBQLN2 mutations are not a frequent cause of amyotrophic lateral sclerosis in ireland. Neurobiology of Aging. 2014;35(1):267.e9-267.e11. 10.1016/j.neurobiolaging.2013.07.023

29. Millecamps S, Corcia P, Cazeneuve C, Boillée S, Seilhean D, Danel-Brunaud V, et al. Mutations in UBQLN2 are rare in French amyotrophic lateral sclerosis. Neurobiology of Aging. 2012;33(4):839.e1-839.e3. 10.1016/j.neurobiolaging.2011.11.010

30. Morgan S, Shatunov A, Sproviero W, Jones AR, Shoai M, Hughes D, et al. A comprehensive analysis of rare genetic variation in amyotrophic lateral sclerosis in the UK. Brain. 2017 Jun 1;140(6):1611–8. 10.1093/brain/awx082

31. Özoğuz A, Uyan Ö, Birdal G, Iskender C, Kartal E, Lahut S, et al. The distinct genetic pattern of ALS in Turkey and novel mutations. Neurobiology of Aging. 2015;36(4):1764.e9-1764.e18. 10.1016/j.neurobiolaging.2014.12.032

32. Synofzik M, Maetzler W, Grehl T, Prudlo J, vom Hagen JM, Haack T, et al. Screening in ALS and FTD patients reveals 3 novel UBQLN2 mutations outside the PXX domain and a pure FTD phenotype. Neurobiology of Aging. 2012;33(12):2949.e13-2949.e17. 10.1016/j.neurobiolaging.2012.07.002

33. Teyssou E, Chartier L, Amador M-D-M, Lam R, Lautrette G, Nicol M, et al. Novel UBQLN2 mutations linked to amyotrophic lateral sclerosis and atypical hereditary spastic paraplegia phenotype through defective HSP70-mediated proteolysis. Neurobiology of Aging. 2017 Oct;58(March):239.e11-239.e20. 10.1016/j.neurobiolaging.2017.06.018

34. Tripolszki K, Gampawar P, Schmidt H, Nagy ZF, Nagy D, Klivényi P, et al. Comprehensive genetic analysis of a Hungarian amyotrophic lateral sclerosis cohort. Frontiers in Genetics. 2019;10(JUL). 10.3389/fgene.2019.00732

35. Ugwu F, Rollinson S, Harris J, Gerhard A, Richardson A, Jones M, et al. A UBQLN2 variant of unknown significance in frontotemporal lobar degeneration. Neurobiology of Aging. 2015 Jan;36(1):546.e15-546.e16. 10.1016/j.neurobiolaging.2014.08.002

36. Vengoechea J, David MP, Yaghi SR, Carpenter L, Rudnicki SA. Clinical variability and female penetrance in X-linked familial FTD/ALS caused by a P506S mutation in UBQLN2. Amyotrophic Lateral Sclerosis and Frontotemporal Degeneration. 2013;14(7–8):615–9. 10.3109/21678421.2013.824001

37. Vildan C, Sule D, Turker B, Hilmi U, Sibel KB. Genetic alterations of C9orf72, SOD1, TARDBP, FUS, and UBQLN2 genes in patients with Amyotrophic Lateral Sclerosis. Cogent Medicine. 2019;6(1):1–10. 10.1080/2331205x.2019.1582400

38. Scotter EL, Smyth L, Bailey JWT, Wong C-H, de Majo M, Vance CA, et al. C9ORF72 and UBQLN2 mutations are causes of amyotrophic lateral sclerosis in New Zealand: a genetic and pathologic study using banked human brain tissue. Neurobiology of Aging. 2017 Jan;49:214.e1-214.e5. 10.1016/j.neurobiolaging.2016.06.019

39. Brettschneider J, van Deerlin VM, Robinson JL, Kwong L, Lee EB, Ali YO, et al. Pattern of ubiquilin pathology in ALS and FTLD indicates presence of C9ORF72 hexanucleotide expansion. Acta Neuropathologica. 2012 Jun 18;123(6):825–39. 10.1007/s00401-012-0970-z

40. Arai T, Hasegawa M, Akiyama H, Ikeda K, Nonaka T, Mori H, et al. TDP-43 is a component of ubiquitin-positive tau-negative inclusions in frontotemporal lobar degeneration and amyotrophic lateral sclerosis. Biochemical and Biophysical Research Communications. 2006;351(3):602–11. 10.1016/j.bbrc.2006.10.093

41. Kwiatkowski TJ, Bosco DA, LeClerc AL, Tamrazian E, Vanderburg CR, Russ C, et al. Mutations in the FUS/TLS gene on chromosome 16 cause familial amyotrophic lateral sclerosis. Science. 2009;323(5918):1205–8. 10.1126/science.1166066

42. Maruyama H, Morino H, Ito H, Izumi Y, Kato H, Watanabe Y, et al. Mutations of optineurin in amyotrophic lateral sclerosis. Nature. 2010;465(7295):223–6. 10.1038/nature08971

43. Neumann M, Sampathu DM, Kwong LK, Truax AC, Micsenyi MC, Chou TT, et al. Ubiquitinated TDP-43 in Frontotemporal Lobar Degeneration and Amyotrophic Lateral Sclerosis. Science. 2006 Oct 6;314(5796):130–3. 10.1126/science.1134108

44. Vance C, Rogelj B, Hortobagyi T, de Vos KJ, Nishimura AL, Sreedharan J, et al. Mutations in FUS, an RNA Processing Protein, Cause Familial Amyotrophic Lateral Sclerosis Type 6. Science. 2009 Feb 27;323(5918):1208–11. 10.1126/science.1165942

45. Waldvogel HJ, Bullock JY, Synek BJ, Curtis MA, van Roon-Mom WMC, Faull RLM. The collection and processing of human brain tissue for research. Cell and Tissue Banking. 2008 Sep 21;9(3):169–79. 10.1007/s10561-008-9068-1

46. Murray HC, Johson K, Sedlock A, Highet B, Dieriks BV, Anekal PV, et al. Lamina-specific immunohistochemical signatures in the olfactory bulb of healthy, Alzheimer's and Parkinson's disease patients. Communications Biology. 2021;

47. Waldvogel HJ, Curtis MA, Baer K, Rees MI, Faull RLM. Immunohistochemical staining of post-mortem adult human brain sections. Nature Protocols. 2007;1(6):2719–32. 10.1038/nprot.2006.354

48. Maric D, Jahanipour J, Li XR, Singh A, Mobiny A, van Nguyen H, et al. Whole-brain tissue mapping toolkit using large-scale highly multiplexed immunofluorescence imaging and deep neural networks. Nature communications. 2021;12(1):1550. 10.1038/s41467-021-21735-x

779 49. Luisier F, Vonesch C, Blu T, Unser M. Fast interscale wavelet denoising of
780 Poisson-corrupted images. Signal Processing. 2010;90(2):415–27.
781 10.1016/j.sigpro.2009.07.009
782 50. Henden L, Wakeham D, Bahlo M. XIBD: Software for inferring pairwise
783 identity by descent on the X chromosome. Bioinformatics. 2016;32(15):2389–
784 91. 10.1093/bioinformatics/btw124
785 51. Li H, Glusman G, Hu H, Shankaracharya, Caballero J, Hubley R, et al.
786 Relationship Estimation from Whole-Genome Sequence Data. PLoS Genetics.
787 2014;10(1). 10.1371/journal.pgen.1004144
788 52. Brettschneider J, del Tredici K, Toledo JB, Robinson JL, Irwin DJ, Grossman
789 M, et al. Stages of pTDP-43 pathology in amyotrophic lateral sclerosis. Annals
790 of Neurology. 2013 Jul;74(1):20–38. 10.1002/ana.23937
791 53. Gorrie GH, Fecto F, Radzicki D, Weiss C, Shi Y, Dong H, et al. Dendritic
792 spinopathy in transgenic mice expressing ALS/dementia-linked mutant
793 UBQLN2. Proceedings of the National Academy of Sciences of the United
794 States of America. 2014;111(40):14524–9. 10.1073/pnas.1405741111
795 54. Liu Y, Yu JT, Sun FR, Ou JR, Qu S ben, Tan L. The clinical and pathological
796 phenotypes of frontotemporal dementia with C9ORF72 mutations. Journal of
797 the Neurological Sciences. 2013;335(1–2):26–35. 10.1016/j.jns.2013.09.013
798 55. Mann DM, Rollinson S, Robinson A, Bennion Callister J, Thompson JC,
799 Snowden JS, et al. Dipeptide repeat proteins are present in the p62 positive
800 inclusions in patients with frontotemporal lobar degeneration and motor
801 neurone disease associated with expansions in C9ORF72. Acta
802 Neuropathologica Communications. 2013;1(1):1. 10.1186/2051-5960-1-68
803 56. Mori K, Weng SM, Arzberger T, May S, Rentzsch K, Kremmer E, et al. The
804 C9orf72 GGGGCC repeat is translated into aggregating dipeptide-repeat
805 proteins in FTLD/ALS. Science. 2013;339(6125):1335–8.
806 10.1126/science.1232927
807 57. Mackenzie IR, Arzberger T, Kremmer E, Troost D, Lorenzl S, Mori K, et al.
808 Dipeptide repeat protein pathology in C9ORF72 mutation cases: Clinico-

pathological correlations. Acta Neuropathologica. 2013;126(6):859–79. 10.1007/s00401-013-1181-y

58. Cohen-Kaplan V, Livneh I, Avni N, Fabre B, Ziv T, Kwon YT, et al. p62- and ubiquitin-dependent stress-induced autophagy of the mammalian 26S proteasome. Proceedings of the National Academy of Sciences of the United States of America. 2016;113(47):E7490–9. 10.1073/pnas.1615455113

59. Seibenhener ML, Babu JR, Geetha T, Wong HC, Krishna NR, Wooten MW. Sequestosome 1/p62 Is a Polyubiquitin Chain Binding Protein Involved in Ubiquitin Proteasome Degradation. Molecular and Cellular Biology. 2004;24(18):8055–68. 10.1128/MCB.24.18.8055-8068.2004

60. Bjørkøy G, Lamark T, Johansen T. p62/SQSTM1: A missing link between protein aggregates and the autophagy machinery. Autophagy. 2006;2(2):138–9. 10.4161/auto.2.2.2405

61. Fecto F, Yan J, Vemula SP, Liu E, Yang Y, Chen W, et al. SQSTM1 Mutations in Familial and Sporadic Amyotrophic Lateral Sclerosis. Archives of Neurology. 2011 Nov 1;68(11):1440. 10.1001/archneurol.2011.250

62. Ravits J, Appel S, Baloh RH, Barohn R, Rix Brooks B, Elman L, et al. Deciphering amyotrophic lateral sclerosis: What phenotype, neuropathology and genetics are telling us about pathogenesis. Amyotrophic Lateral Sclerosis and Frontotemporal Degeneration. 2013 May 16;14(sup1):5–18. 10.3109/21678421.2013.778548

63. Nguyen HP, van Broeckhoven C, van der Zee J. ALS Genes in the Genomic Era and their Implications for FTD. Trends in Genetics. 2018;34(6):404–23. 10.1016/j.tig.2018.03.001

64. Taylor JP, Brown RH, Cleveland DW. Decoding ALS: From genes to mechanism. Nature. 2016;539(7628):197–206. 10.1038/nature20413

65. Ling S, Polymenidou M, Cleveland DW. Converging Mechanisms in ALS and FTD: Disrupted RNA and Protein Homeostasis. Neuron. 2013 Aug;79(3):416–38. 10.1016/j.neuron.2013.07.033

66. Mori K, Arzberger T, Grässer FA, Gijselinck I, May S, Rentzsch K, et al. Bidirectional transcripts of the expanded C9orf72 hexanucleotide repeat are

translated into aggregating dipeptide repeat proteins. Acta Neuropathologica. 2013;126(6):881–93. 10.1007/s00401-013-1189-3

67. Shibata N, Hirano A, Kobayashi M, Siddique T, Deng H-X, Hung W-Y, et al. Intense Superoxide Dismutase-1 Immunoreactivity in Intracytoplasmic Hyaline Inclusions of Familial Amyotrophic Lateral Sclerosis with Posterior Column Involvement. Journal of Neuropathology and Experimental Neurology. 1996 Apr;55(4):481–90. 10.1097/00005072-199604000-00011

68. Bruijn LI, Houseweart MK, Kato S, Anderson KL, Anderson SD, Ohama E, et al. Aggregation and Motor Neuron Toxicity of an ALS-Linked SOD1 Mutant Independent from Wild-Type SOD1. Science. 1998 Sep 18;281(5384):1851–4. 10.1126/science.281.5384.1851

69. Keith JL, Swinkin E, Gao A, Alminawi S, Zhang M, Mcgoldrick P, et al. Neuropathologic description of CHCHD10 mutated amyotrophic lateral sclerosis. Neurology: Genetics. 2020;6(1). 10.1212/NXG.0000000000000394

70. Smith BN, Topp SD, Fallini C, Shibata H, Chen H-J, Troakes C, et al. Mutations in the vesicular trafficking protein annexin A11 are associated with amyotrophic lateral sclerosis. Science Translational Medicine. 2017 May 3;9(388):eaad9157. 10.1126/scitranslmed.aad9157

71. Smith BN, Vance C, Scotter EL, Troakes C, Wong CH, Topp S, et al. Novel mutations support a role for Profilin 1 in the pathogenesis of ALS. Neurobiology of Aging. 2015;36(3):1602.e17-1602.e27. 10.1016/j.neurobiolaging.2014.10.032

72. Teyssou E, Takeda T, Lebon V, Boillée S, Doukouré B, Bataillon G, et al. Mutations in SQSTM1 encoding p62 in amyotrophic lateral sclerosis: genetics and neuropathology. Acta Neuropathologica. 2013 Apr 17;125(4):511–22. 10.1007/s00401-013-1090-0

73. Hirsch-Reinshagen V, Pottier C, Nicholson AM, Baker M, Hsiung GYR, Krieger C, et al. Clinical and neuropathological features of ALS/FTD with TIA1 mutations. Acta neuropathologica communications. 2017;5(1):96. 10.1186/s40478-017-0493-x

74. Tada M, Doi H, Koyano S, Kubota S, Fukai R, Hashiguchi S, et al. Matrin 3 Is a Component of Neuronal Cytoplasmic Inclusions of Motor Neurons in Sporadic Amyotrophic Lateral Sclerosis. American Journal of Pathology. 2018;188(2):507–14. 10.1016/j.ajpath.2017.10.007

75. van Deerlin VM, Leverenz JB, Bekris LM, Bird TD, Yuan W, Elman LB, et al. TARDBP mutations in amyotrophic lateral sclerosis with TDP-43 neuropathology: a genetic and histopathological analysis. The Lancet Neurology. 2008 May;7(5):409–16. 10.1016/S1474-4422(08)70071-1

76. Tan RH, Kril JJ, Fatima M, McGeachie A, McCann H, Shepherd C, et al. TDP-43 proteinopathies: Pathological identification of brain regions differentiating clinical phenotypes. Brain. 2015;138(10):3110–22. 10.1093/brain/awv220

77. Brettschneider J, del Tredici K, Irwin DJ, Grossman M, Robinson JL, Toledo JB, et al. Sequential distribution of pTDP-43 pathology in behavioral variant frontotemporal dementia (bvFTD). Acta Neuropathologica. 2014;127(3):423–39. 10.1007/s00401-013-1238-y

78. Balendra R, Isaacs AM. C9orf72-mediated ALS and FTD: multiple pathways to disease. Nature Reviews Neurology. 2018;14(9):544–58. 10.1038/s41582-018-0047-2

79. van Blitterswijk M, DeJesus-Hernandez M, Rademakers R. How do C9ORF72 repeat expansions cause amyotrophic lateral sclerosis and frontotemporal dementia. Current Opinion in Neurology. 2012 Dec;25(6):689–700. 10.1097/WCO.0b013e32835a3efb

80. DeJesus-Hernandez M, Mackenzie IR, Boeve BF, Boxer AL, Baker M, Rutherford NJ, et al. Expanded GGGGCC Hexanucleotide Repeat in Noncoding Region of C9ORF72 Causes Chromosome 9p-Linked FTD and ALS. Neuron. 2011;72(2):245–56. 10.1016/j.neuron.2011.09.011

81. Murray ME, Dejesus-Hernandez M, Rutherford NJ, Baker M, Duara R, Graff-Radford NR, et al. Clinical and neuropathologic heterogeneity of c9FTD/ALS associated with hexanucleotide repeat expansion in C9ORF72. Acta Neuropathologica. 2011;122(6):673–90. 10.1007/s00401-011-0907-y

82. McEachin ZT, Gendron TF, Raj N, García-Murias M, Banerjee A, Purcell RH, et al. Chimeric Peptide Species Contribute to Divergent Dipeptide Repeat Pathology in c9ALS/FTD and SCA36. Neuron. 2020;107(2):292-305.e6. 10.1016/j.neuron.2020.04.011

83. Freibaum BD, Taylor JP. The Role of Dipeptide Repeats in C9ORF72-Related ALS-FTD. Frontiers in Molecular Neuroscience. 2017;10(February):1–9. 10.3389/fnmol.2017.00035

84. Lee YB, Baskaran P, Gomez-Deza J, Chen HJ, Nishimura AL, Smith BN, et al. C9orf72 poly GA RAN-translated protein plays a key role in amyotrophic lateral sclerosis via aggregation and toxicity. Human Molecular Genetics. 2017;26(24):4765–77. 10.1093/hmg/ddx350

85. Nonaka T, Masuda-Suzukake M, Hosokawa M, Shimozawa A, Hirai S, Okado H, et al. C9ORF72 dipeptide repeat poly-GA inclusions promote intracellular aggregation of phosphorylated TDP-43. Human Molecular Genetics. 2018;27(15):2658–70. 10.1093/hmg/ddy174

86. Lindsay RD, Scheibel AB. Quantitative analysis of dendritic branching pattern of granular cells from human dentate gyrus. Experimental Neurology. 1976 Aug;52(2):295–310. 10.1016/0014-4886(76)90173-4

87. Amaral DG, Scharfman HE, Lavenex P. The dentate gyrus: fundamental neuroanatomical organization (dentate gyrus for dummies). Progress in Brain Research. 2007;163:3–22. 10.1016/S0079-6123(07)63001-5

88. May S, Hornburg D, Schludi MH, Arzberger T, Rentzsch K, Schwenk BM, et al. C9orf72 FTLD/ALS-associated Gly-Ala dipeptide repeat proteins cause neuronal toxicity and Unc119 sequestration. Acta Neuropathologica. 2014;128(4):485–503. 10.1007/s00401-014-1329-4

89. Gupta R, Lan M, Mojsilovic-Petrovic J, Choi WH, Safren N, Barmada S, et al. The proline/arginine dipeptide from hexanucleotide repeat expanded C9ORF72 inhibits the proteasome. eNeuro. 2017;4(1). 10.1523/ENEURO.0249-16.2017

90. Zhang YJ, Gendron TF, Grima JC, Sasaguri H, Jansen-West K, Xu YF, et al. C9ORF72 poly(GA) aggregates sequester and impair HR23 and

nucleocytoplasmic transport proteins. Nature Neuroscience. 2016;19(5):668–77. 10.1038/nn.4272

91. van Blitterswijk M, Gendron TF, Baker MC, DeJesus-Hernandez M, Finch NA, Brown PH, et al. Novel clinical associations with specific C9ORF72 transcripts in patients with repeat expansions in C9ORF72. Acta Neuropathologica. 2015 Dec 5;130(6):863–76. 10.1007/s00401-015-1480-6

92. Webster CP, Smith EF, Bauer CS, Moller A, Hautbergue GM, Ferraiuolo L, et al. The C9orf72 protein interacts with Rab1a and the ULK 1 complex to regulate initiation of autophagy . The EMBO Journal. 2016;35(15):1656–76. 10.15252/embj.201694401

93. Wang M, Wang H, Tao Z, Xia Q, Hao Z, Prehn JHM, et al. C9orf72 associates with inactive Rag GTPases and regulates mTORC1-mediated autophagosomal and lysosomal biogenesis. Aging Cell. 2020;19(4):1–14. 10.1111/acel.13126

94. Boivin M, Pfister V, Gaucherot A, Ruffenach F, Negroni L, Sellier C, et al. Reduced autophagy upon C9ORF72 loss synergizes with dipeptide repeat protein toxicity in G4C2 repeat expansion disorders. The EMBO Journal. 2020;39(4):1–15. 10.15252/embj.2018100574

95. Zhu Q, Jiang J, Gendron TF, McAlonis-Downes M, Jiang L, Taylor A, et al. Reduced C9ORF72 function exacerbates gain of toxicity from ALS/FTD-causing repeat expansion in C9orf72. Nature Neuroscience. 2020;23(May). 10.1038/s41593-020-0619-5

96. Beckers J, Tharkeshwar AK, van Damme P. C9orf72 ALS-FTD: recent evidence for dysregulation of the autophagy-lysosome pathway at multiple levels. Autophagy. 2021;00(00):1–17. 10.1080/15548627.2021.1872189

97. Sellier C, Campanari M, Julie Corbier C, Gaucherot A, Kolb-Cheynel I, Oulad-Abdelghani M, et al. Loss of C9ORF72 impairs autophagy and synergizes with polyQ Ataxin-2 to induce motor neuron dysfunction and cell death. The EMBO Journal. 2016;35(12):1276–97. 10.15252/embj.201593350

98. Renaud L, Picher-Martel V, Codron P, Julien J. Key role of UBQLN2 in pathogenesis of amyotrophic lateral sclerosis and frontotemporal dementia.

961 Acta Neuropathologica Communications. 2019 Dec 18;7(1):103.
962 10.1186/s40478-019-0758-7
963 99. Zhang KY, Yang S, Warraich ST, Blair IP. Ubiquilin 2: A component of the
964 ubiquitin-proteasome system with an emerging role in neurodegeneration.
965 International Journal of Biochemistry and Cell Biology. 2014;50(1):123–6.
966 10.1016/j.biocel.2014.02.018
967 100. Sharkey LM, Sandoval-Pistorius SS, Moore SJ, Gerson JE, Komlo R, Fischer
968 S, et al. Modeling UBQLN2-mediated neurodegenerative disease in mice:
969 Shared and divergent properties of wild type and mutant UBQLN2 in phase
970 separation, subcellular localization, altered proteostasis pathways, and
971 selective cytotoxicity. Neurobiology of Disease. 2020;143(June).
972 10.1016/j.nbd.2020.105016
973 101. Al-Sarraj S, King A, Troakes C, Smith B, Maekawa S, Bodi I, et al. p62
974 positive, TDP-43 negative, neuronal cytoplasmic and intranuclear inclusions in
975 the cerebellum and hippocampus define the pathology of C9orf72-linked
976 FTLD and MND/ALS. Acta Neuropathologica. 2011 Dec 19;122(6):691–702.
977 10.1007/s00401-011-0911-2
978 102. Piras A, Collin L, Grüninger F, Graff C, Rönnbäck A. Autophagic and
979 lysosomal defects in human tauopathies: analysis of post-mortem brain from
980 patients with familial Alzheimer disease, corticobasal degeneration and
981 progressive supranuclear palsy. Acta neuropathologica communications.
982 2016;4:22. 10.1186/s40478-016-0292-9
983 103. Babu JR, Geetha T, Wooten MW. Sequestosome 1/p62 shuttles
984 polyubiquitinated tau for proteasomal degradation. Journal of Neurochemistry.
985 2005;94(1):192–203. 10.1111/j.1471-4159.2005.03181.x
986 104. Zatloukal K, Stumptner C, Fuchsbichler A, Heid H, Schnoelzer M, Kenner L,
987 et al. P62 Is a Common Component of Cytoplasmic Inclusions in Protein
988 Aggregation Diseases. American Journal of Pathology. 2002;160(1):255–63.
989 10.1016/S0002-9440(10)64369-6

105. Kuusisto E, Salminen A, Alafuzoff I. Ubiquitin-binding protein p62 is present in neuronal and glial inclusions in human tauopathies and synucleinopathies. NeuroReport. 2001;12(10):2085–90. 10.1097/00001756-200107200-00009

106. Richards S, Aziz N, Bale S, Bick D, Das S, Gastier-Foster J, et al. Standards and guidelines for the interpretation of sequence variants: A joint consensus recommendation of the American College of Medical Genetics and Genomics and the Association for Molecular Pathology. Genetics in Medicine. 2015;17(5):405–24. 10.1038/gim.2015.30

107. Ramstetter MD, Dyer TD, Lehman DM, Curran JE, Duggirala R, Blangero J, et al. Benchmarking relatedness inference methods with genome-wide data from thousands of relatives. Genetics. 2017;207(1):75–82. 10.1534/genetics.117.1122

Tables

Table 1. IBD segments inferred over *UBQLN2* on the X chromosome (chromosome 23).

Individual 1		Individual 2					
Family ID	**Pedigree ID**	**Family ID**	**Individual ID**	**StartSNP**	**EndSNP**	**Start Pos(bp)**	**End Pos(bp)**
FALS5	III:8	FALS5	IV:9	rs17330993	rs11156600	2779749	154440161
FALS5	III:8	FALS5	IV:18[a]	rs7062445	rs6423133	19650411	123608292
FALS5	III:8	FALS14	III:2	rs952836	rs17315029	40344087	129605268
FALS5	IV:9	FALS5	IV:18	rs6628597	rs6423133	31382037	123608292
FALS5	IV:9	FALS14	III:2	rs952836	rs17277770	40344087	132774456
FALS5	IV:18	FALS14	III:2	rs952836	rs6423133	40344087	123608292

[a] FALS5 IV:18 is also referred to as MN17 in this report.

Table 2. Estimated degree of relatedness and fraction of genome with zero, one, and two alleles identical-by-descent (IBD) between all samples in *UBQLN2* p.T487I-linked families FALS5 and FALS14.

	Individual 1		Individual 2					
	Family ID	**Pedigree ID**	**Family ID**	**Individual ID**	**Fraction IBD=0**	**Fraction IBD=1**	**Fraction IBD=2**	**Degree[a]**
Intra-family	FALS5	III:8	FALS5	IV:9	0.529	0.471	0	2
	FALS5	III:8	FALS5	IV:18[b]	0.529	0.471	0	2
	FALS5	IV:9	FALS5	IV:18	0.751	0.249	0	3
	FALS14	II:1	FALS14	III:2	0.515	0.485	0	2
Inter-family	FALS5	III:8	FALS14	II:1	0.877	0.123	0	4
	FALS5	III:8	FALS14	III:2	0.927	0.073	0	5
	FALS5	IV:9	FALS14	II:1	0.942	0.058	0	5
	FALS5	IV:9	FALS14	III:2	0.948	0.052	0	5
	FALS5	IV:18	FALS14	II:1	0.926	0.074	0	5
	FALS5	IV:18	FALS14	III:2	0.948	0.052	0	5

[a] Degrees of relatedness as per [107]:

2 – Grandparent-grandchild, Avuncular, Half-sibling

3 – First cousin, Great-grandparent, Grand-avuncular

4 – First cousin once removed, GG-grandparent

5 – Second cousin, First cousin twice removed

[b] FALS5 IV:18 is also referred to as MN17 in this report.

Figure legends

Figure 1. Ubiquilin 2 labelling in previous studies fails to discriminate between *UBQLN2*-linked and other genotypes of ALS/FTD. Previously published immunohistochemical analyses of the spinal cord, and hippocampus molecular layer (ML), granule cell layer (GCL), and cornus ammonus (CA) regions fail to discriminate between *UBQLN2*-linked ALS/FTD and ALS/FTD with other genotypes. Key shown within figure. Spinal cord ubiquilin 2 pathology (green) is reported to be present when ubiquilin 2 is either mutant or wildtype, occurring in *UBQLN2*-linked and *C9ORF72*-linked ALS/FTD, "ALS-dementia" (later confirmed to be *C9ORF72*-positive), *FUS*-linked ALS, and sporadic ALS (sALS). Spinal cord ubiquilin 2 pathology is found together with ubiquitin (orange), p62 (dark pink), TDP-43 (yellow), and FUS (blue) aggregates. Similarly, hippocampal ubiquilin 2 pathology is reported when ubiquilin 2 is either mutant or wildtype; being present in the molecular layer in *UBQLN2*-linked and *C9ORF72*-linked ALS/FTD (including "ALS-dementia") but not in sALS; and in the granule cell layer in *C9ORF72*-linked ALS/FTD (including "ALS-dementia"). Hippocampal granule cell layer ubiquilin 2 pathology is found together with dipeptide repeats (DPRs, pale red) with or without TDP-43; but is variably present in *UBQLN2*-linked ALS/FTD and sALS. In the hippocampal CA regions, ubiquilin 2 is present in *UBQLN2*-linked and *C9ORF72*-linked ALS/FTD (including "ALS-dementia"). Hippocampal CA region ubiquilin 2 pathology is found together with DPRs, ubiquitin and p62.

Figure 2. Ubiquilin 2 and pTDP-43 pathology in the hippocampal granule cell layer and molecular layer. Sections from 5 sporadic ALS cases (**A-F**) demonstrated variable perinuclear pTDP-43 aggregate load in the granule cell layer (**A-F, A1-F1**, white arrowheads). These aggregates were all devoid of ubiquilin 2 co-labelling. All *UBQLN2*-linked ALS/FTD cases (**G-J**) showed ubiquilin 2-positive (**G1, H1, I1', J2',** green arrowheads), pTDP-43-negative (**G2, H2, I2", J2"**) punctate aggregates in the molecular layer, with the exception of one aggregate found in ALS+FTD case V:7 – p.T487I which showed co-deposition of both proteins in this region (**I**, white arrow). ALS+FTD cases V:7 – p.T487I and p.P506S showed rare granule cell layer pTDP-43 aggregates independent of ubiquilin 2 (**I2', I2", J3', J3"**, white arrowheads). Only in p.P506S were the numerous

compact pTDP-43 aggregates found in the granule cell layer co-localised with ubiquilin 2 (**J1,** unfilled green arrowheads). *C9ORF72*-linked ALS cases MN2, MN18, and MN23 (**K-L**), were devoid of pTDP-43 pathology in the molecular (**K1, L1, M1,** green arrowheads) and granule cell layers (**K2, L2, M2,** green arrowheads) but showed wispy, and stellate ubiquilin 2 aggregates in these layers, respectively. Similarly, dendritic ubiquilin 2 inclusions were observed in the molecular layer of *C9ORF72*-linked ALS case MN28, aggregating alone (**N2', N2"**). Unique to MN28 were granule cell layer perinuclear pTDP-43 inclusions, often found aggregating independently (**N3"**, white arrowheads). Stellate ubiquilin 2 aggregates were observed in the granule cell layer which very rarely co-localised with pTDP-43 (**N1**, unfilled green arrowhead) or more commonly alone (**N1, N3'**, green arrowhead). Scale bar in main images, 50 µm; in insets A1-F1, J1, N1, 10 µm; all other zooms, 5 µm.

Figure 3. Ubiquilin 2 and DPR pathology in hippocampal granule cell layer and molecular layer. All *UBQLN2*-linked cases (**A-D**) displayed characteristic molecular layer ubiquilin 2 aggregates (**A1-D1**), with granule cell layer ubiquilin 2 aggregates only seen in case p.P506S (**D2**). All *UBQLN2*-linked cases were DPR-negative (**A1'-D1', A1"-D1"**). In *C9ORF72*-linked ALS cases (**E-H**), skein-like ubiquilin 2 aggregates in the molecular layer were DPR-negative (**E1'-H1', E1"-H1"**), but granule cell layer ubiquilin 2 aggregates always co-localised with either polyGA alone (**E2'-H2', E2"-H2"**, yellow arrowheads) or both polyGA and polyGP proteins (not shown). Pink arrowheads indicate co-localised DPRs not ubiquilin 2-labelled (**E2-H2"**). Scale bar in main images, 50 µm; insets, 10 µm. Super-resolution STED microscopy of co-localised ubiquilin 2-polyGA aggregates in *C9ORF72*-linked ALS case MN28 demonstrated ubiquilin 2 aggregation around a core of aggregated polyGA (**I-I"**) or polyGA enmeshed with and encircling ubiquilin 2 (**J-J"**). Scale bar, 1 µm.

Figure 4. Mutant ubiquilin 2 was p62 positive in hippocampal molecular layer. Four *UBQLN2*-linked ALS/FTD cases (**A-D**) showed abundant, compact ubiquilin 2 aggregates in the molecular layer, predominantly co-localised with p62 (**A-D"**, orange arrowheads) but occasionally not (**A-D",** green arrowheads). *C9ORF72*-linked ALS case MN28 (**E**)

showed analogous ubiquilin 2 aggregates in the molecular layer but these were mostly devoid of p62 (**E-E"**, green arrowheads), with infrequent p62 co-labelling of larger ubiquilin 2 aggregates (**E', E"**, orange arrowhead). Maximum intensity Z-projections with orthogonal planes of the molecular layer confirmed that almost all mutant ubiquilin 2 aggregates in *UBQLN2*-linked ALS+FTD case p.P506S were compact and p62-labelled (**F**, white dotted outline, z= 22.25 µm) with very few ubiquilin 2 aggregates that were p62-negative (**F,** green arrowheads), while the majority of wildtype ubiquilin 2 in *C9ORF72*-linked case MN28 were wispy and p62-negative (**G,** white dotted outline, z= 13 µm). Scale bar, 10 µm.

Figure 5. Combined pTDP-43, ubiquilin 2, p62, and dipeptide repeat protein immunohistochemical staining discriminates between sporadic and *C9ORF72*-linked ALS, and *UBQLN2*-linked ALS/FTD. Combined immunohistochemical analyses of the hippocampal molecular layer (ML) and granule cell layer (GCL) fully discriminate between *UBQLN2*-linked ALS/FTD, *C9ORF72*-linked ALS, and ALS with other genotypes. Key shown within figure. pTDP-43 pathology (boxed '+' symbol on yellow box) is present in the hippocampal granule cell layer in some sALS cases (6/19, 32%). Ubiquilin 2 pathology (pale pink) is present in the hippocampus when ubiquilin 2 is mutant (*UBQLN2*-linked ALS/FTD) and when wildtype (*C9ORF72*-linked ALS). Blue outlines indicate unique aggregation features of *C9ORF72*-linked ALS and *UBQLN2*-linked ALS/FTD hippocampal pathology. Wildtype ubiquilin 2 in *C9ORF72*-linked ALS molecular layer is p62-negative, and associated with granule cell layer polyGA, polyGP, and ubiquilin 2-positive aggregates that were pTDP-43 positive in only one case, and even then only rarely. Mutant ubiquilin 2 in *UBQLN2*-linked ALS/FTD molecular layer is p62-positive, and associated with granule cell layer pTDP-43 aggregates only in some cases and which may or may not be ubiquilin 2-labelled.

Figure 6. Schematic representation of the hippocampal neuropathological signature defining *UBQLN2*-linked ALS. In *UBQLN2*-linked ALS/FTD cases without hippocampal pTDP-43 proteinopathy, mutant ubiquilin 2 is punctate, p62 positive, and forms aggregates exclusively in the molecular layer (cases p.P497H and MN17 – p.T487I). In *UBQLN2*-

linked ALS/FTD cases with hippocampal pTDP-43 proteinopathy, in addition to punctate p62-positive ubiquilin 2 aggregates in the molecular layer, there are granule cell layer pTDP-43 aggregates that are either; frequent and ubiquilin 2-labelled (case p.P506S), or rare and ubiquilin 2-negative (case V:7-p.T487I), suggesting a pathological cascade in which granule cell layer pTDP-43 aggregates provide a scaffold around which mutant ubiquilin 2 can aggregate. Image created in Biorender.com

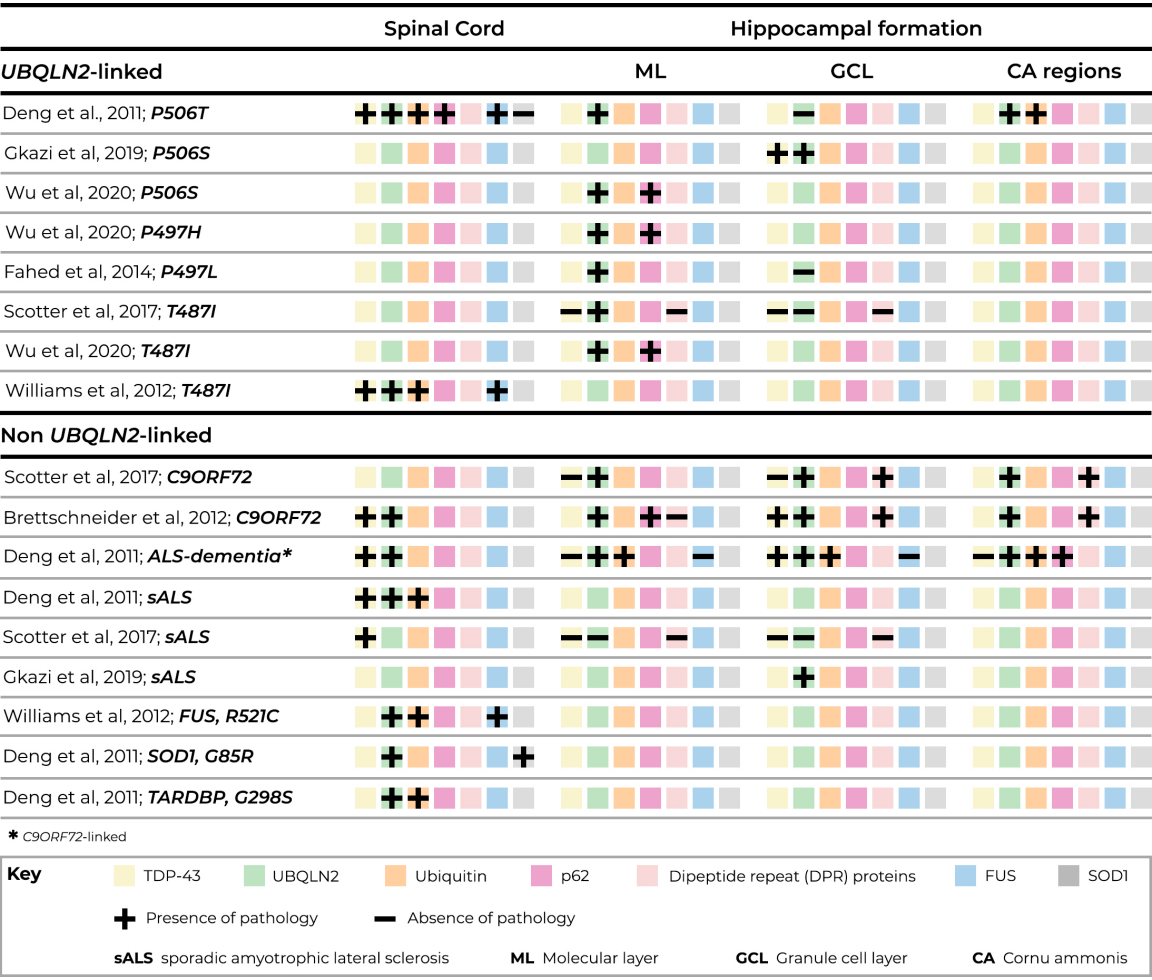
Spinal Cord
Hippocampal formation
UBQLN2-linked
ML
GCL
CA regions
Deng et al., 2011; ***P506T***
Gkazi et al, 2019; ***P506S***
Wu et al, 2020; ***P506S***
Wu et al, 2020; ***P497H***
Fahed et al, 2014; ***P497L***
Scotter et al, 2017; ***T487I***
Wu et al, 2020; ***T487I***
Williams et al, 2012; ***T487I***
Non *UBQLN2*-linked
Scotter et al, 2017; ***C9ORF72***
Brettschneider et al, 2012; ***C9ORF72***
Deng et al, 2011; ***ALS-dementia****
Deng et al, 2011; ***sALS***
Scotter et al, 2017; ***sALS***
Gkazi et al, 2019; ***sALS***
Williams et al, 2012; ***FUS, R521C***
Deng et al, 2011; ***SOD1, G85R***
Deng et al, 2011; ***TARDBP, G298S***
* *C9ORF72*-linked
Key
TDP-43
UBQLN2
Ubiquitin
p62
Dipeptide repeat (DPR) proteins
FUS
SOD1
Presence of pathology
Absence of pathology
sALS sporadic amyotrophic lateral sclerosis
ML Molecular layer
GCL Granule cell layer
CA Cornu ammonis

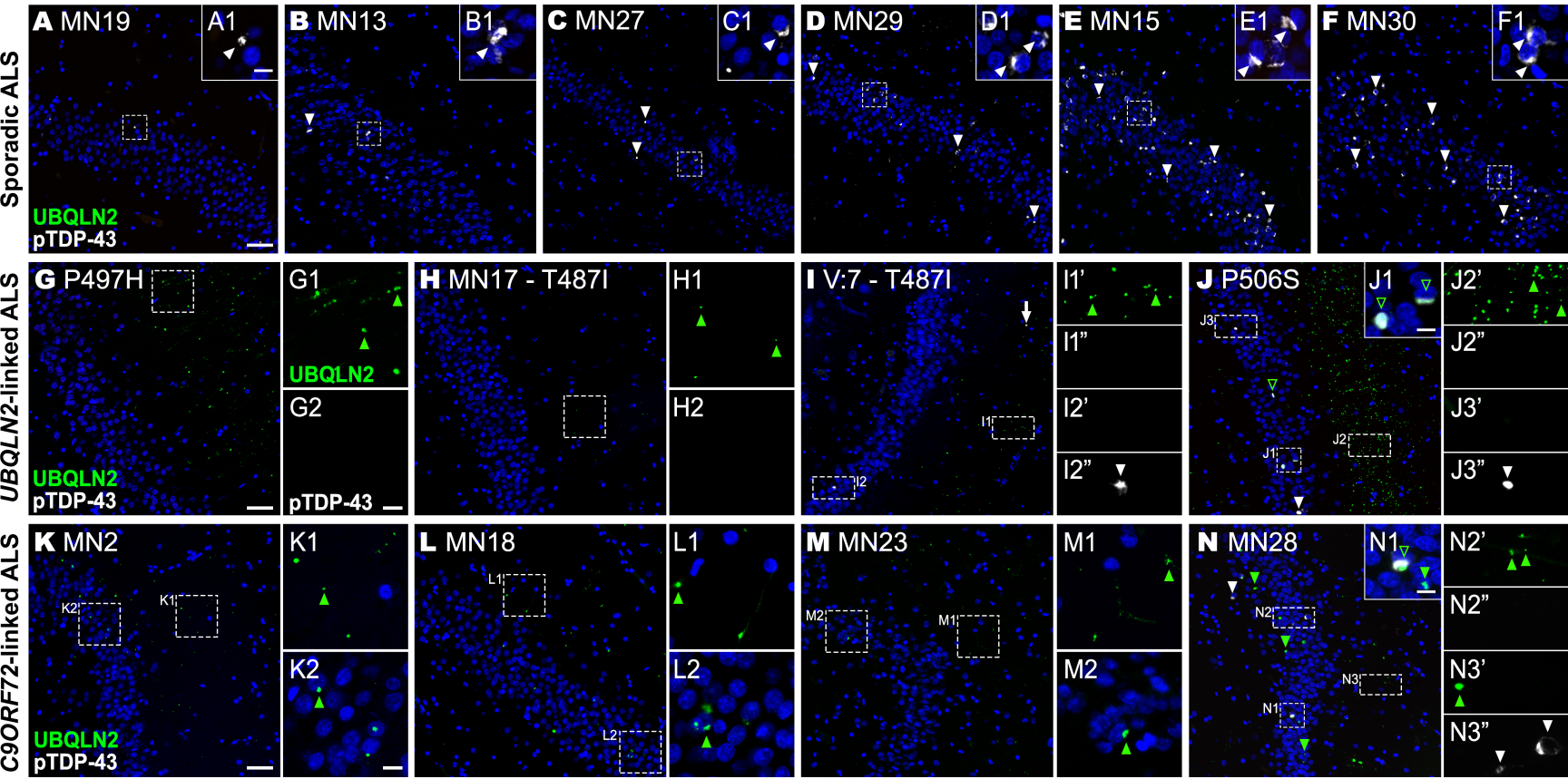
Sporadic ALS
UBQLN2-linked ALS
C9ORF72-linked ALS
A MN19
A1
B MN13
B1
C MN27
C1
D MN29
D1
E MN15
E1
F MN30
F1
UBQLN2
pTDP-43
G P497H
G1
G2
H MN17 - T487I
H1
H2
I V:7 - T487I
I1
I2
I1'
I1"
I2'
I2"
J P506S
J1
J2
J3
J1'
J2'
J2"
J3'
J3"
K MN2
K1
K2
L MN18
L1
L2
M MN23
M1
M2
N MN28
N1
N2
N3
N1'
N2'
N2"
N3'
N3"

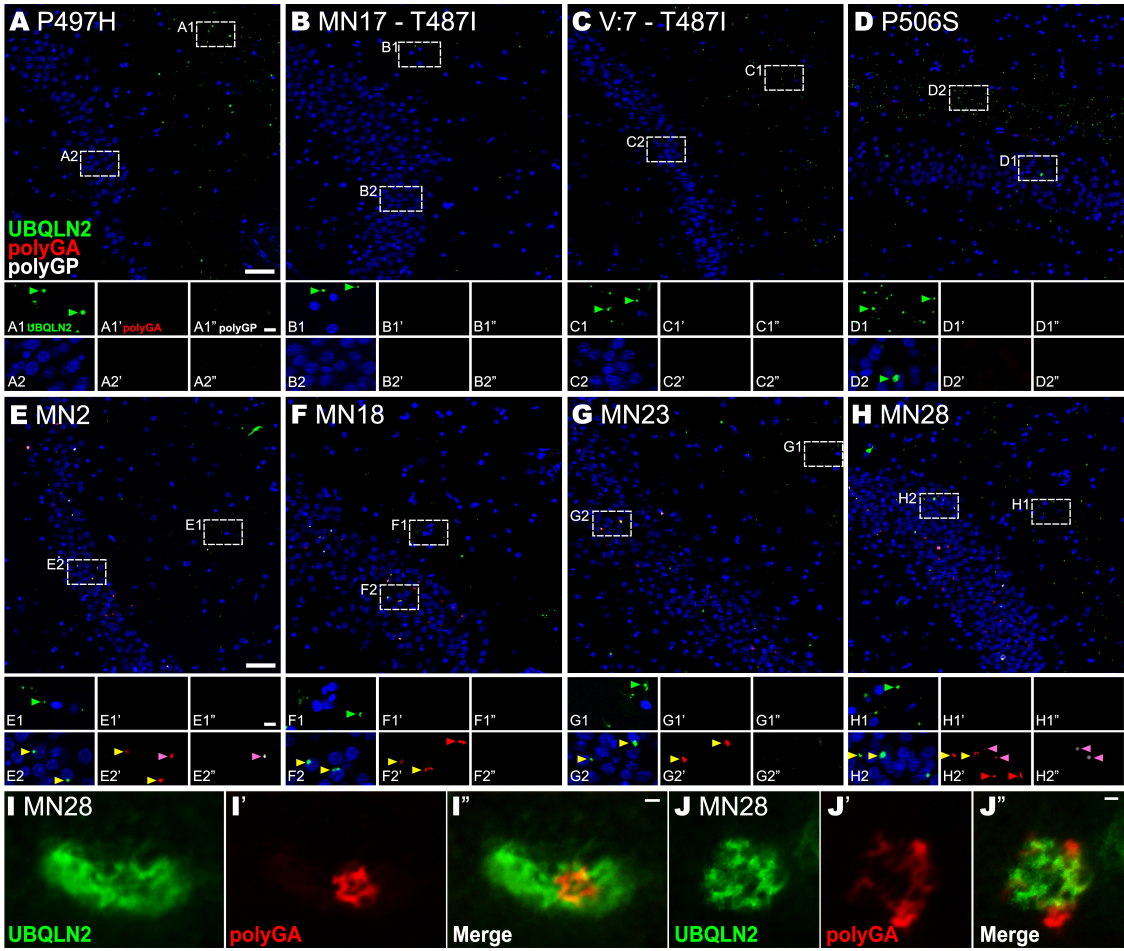
UBQLN2-linked ALS
C9ORF72-linked ALS
A P497H
B MN17 - T487I
C V:7 - T487I
D P506S
E MN2
F MN18
G MN23
H MN28
I MN28
J MN28
UBQLN2
polyGA
polyGP
Merge

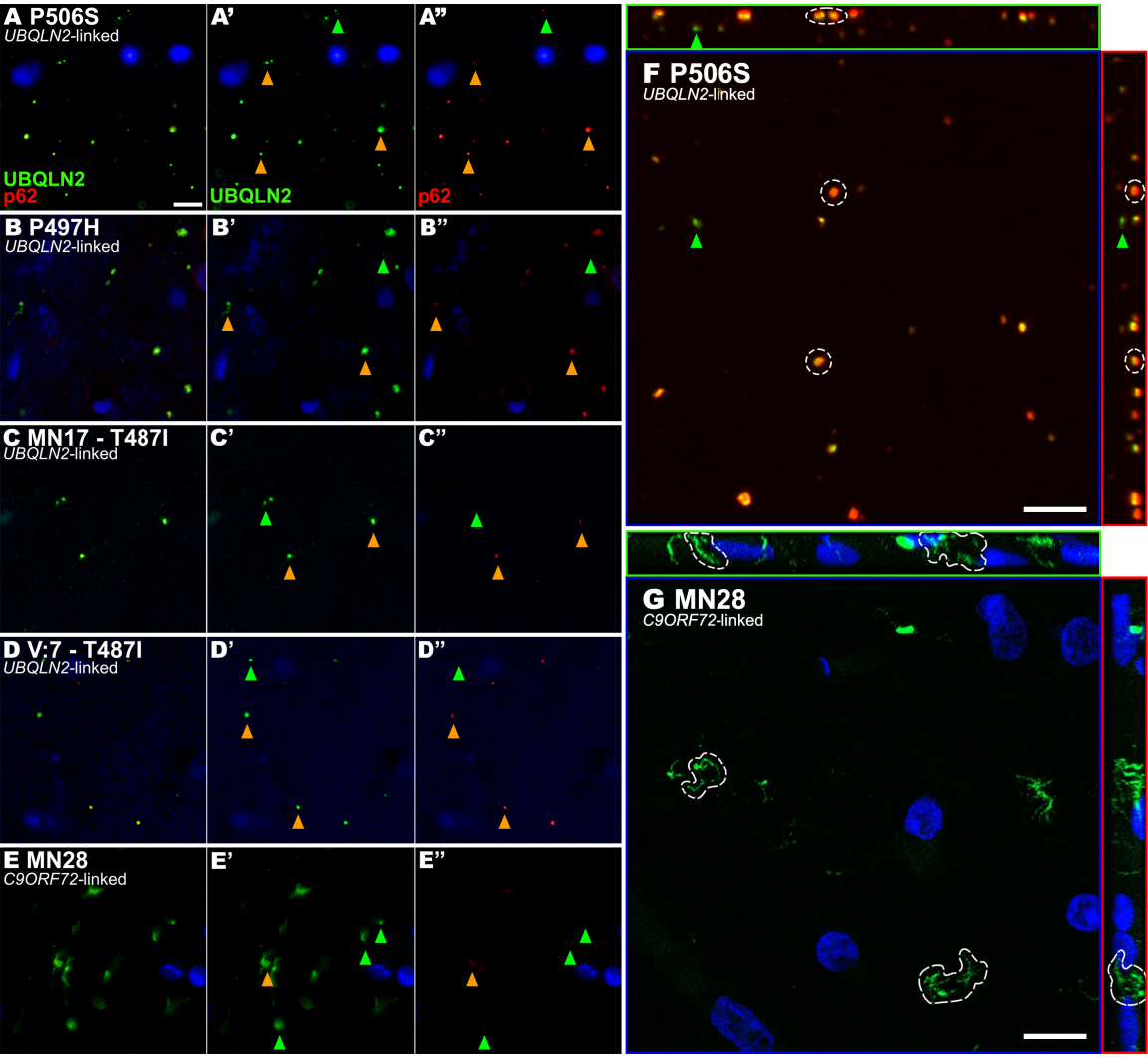
A P506S
UBQLN2-linked
UBQLN2
p62
A'
UBQLN2
A"
p62
B P497H
UBQLN2-linked
B'
B"
C MN17 - T487I
UBQLN2-linked
C'
C"
D V:7 - T487I
UBQLN2-linked
D'
D"
E MN28
C9ORF72-linked
E'
E"
F P506S
UBQLN2-linked
G MN28
C9ORF72-linked

Genetic classification	Case & mutation	Diagnosis	Pathological co-localisation	
			ML	GCL
Neurologically Normal (n=5)	H211	NN		
	H230	NN		
	H238	NN		
	H239	NN		
	H247	NN		
Unknown Familial ALS (n=3)	MN11	MND-ALS		
	MN14	Probable MND-ALS		
	MN21	MND-ALS		
SOD1-linked ALS (n=1)	MN24; E101G	MND-ALS		
Sporadic ALS (n=19)	MN4	MND-ALS		
	MN8	MND-ALS		
	MN9	MND-ALS		
	MN10	MND-ALS		
	MN12	MND-ALS		
	MN20	MND-ALS		
	MN22	MND-ALS		
	MN25	MND-ALS		
	MN5	MND-ALS		
	MN6	MND-ALS		
	MN16	MND-ALS		
	MN26	MND-ALS		
	MN19	MND-ALS		+
	MN13	MND-ALS		+
	MN27	MND-ALS/LBD-bs		+
	MN29	MND-ALS		+
	MN15	MND-ALS + FTD		+
	MN30	MND-ALS		+
C9ORF72-linked ALS (n=4)	MN2	MND-ALS	+	+ + +
	MN18	MND-ALS	+	+ + +
	MN23	MND-ALS	+	+ + +
	MN28	MND-ALS	+	+ + + +
UBQLN2-linked ALS (n=4)	MN17 - T487I	MND-ALS + FTD	+ +	
	P497H	MND-ALS	+ +	
	V7 - T487I	MND-ALS + FTD	+ +	+
	P506S	MND-ALS + FTD	+ +	+ +

Key pTDP-43 UBQLN2 p62 polyGA polyGP Stage 4 ALS

\+ Presence of pathology − Absence of pathology **ML** Molecular layer **GCL** Granular cell layer

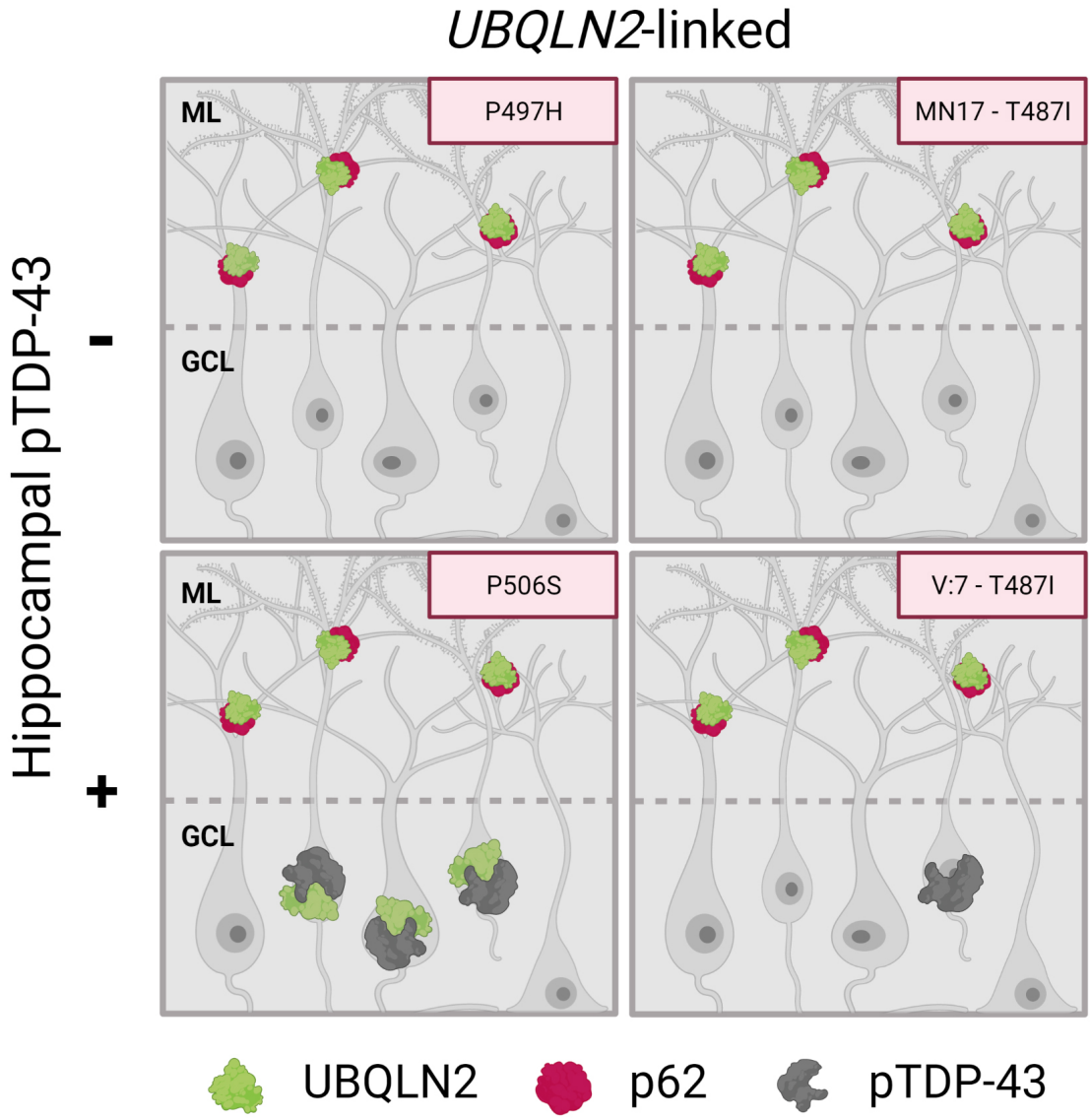
UBQLN2-linked
Hippocampal pTDP-43
-
+
ML
GCL
P497H
MN17 - T487I
P506S
V:7 - T487I
UBQLN2
p62
pTDP-43